Large methane emissions from tree stems complicate the wetland methane budget

L. C. Jeffrey[1], C. A. Moras[1], D. R. Tait[1], S. G. Johnston[1], M. Call[1], J. Z. Sippo[1], N. C. Jeffrey, D. Laicher-Edwards[1] & D. T. Maher[1]

[1]Faculty of Science and Engineering, Southern Cross University, Military Rd, East Lismore, NSW 2480.

Corresponding author: Luke C. Jeffrey (luke.jeffrey@scu.edu.au)

3 key points

1. Bi-monthly tree stem methane emissions were quantified in a subtropical wetland *Melaleuca quinquenervia* forest over an annual cycle.
2. Dynamic tree stem methane emissions spanned six orders of magnitude and were largely driven by changes in the water table height.
3. Tree stems contributed 28-68 % of the annual wetland methane flux, therefore an important component of forested-wetland methane budgets.

Abstract

Our understanding of tree stem methane (CH_4) emissions is evolving rapidly. Few studies have combined seasonal measurements of soil, water and tree stem CH_4 emissions from forested wetlands, inhibiting our capacity to constrain the tree stem CH_4 flux contribution to total wetland CH_4 flux. Here we present annual data from a subtropical freshwater Melaleuca quinquenervia wetland forest, spanning an elevational topo-gradient (Lower, Transitional and Upper zones). Eight field-campaigns captured an annual hydrological flood-dry-flood cycle, measuring stem fluxes on 30 trees, from four stem heights, and up to 30 adjacent soil or water CH_4 fluxes per campaign. Tree stem CH_4 fluxes ranged several orders of magnitude between hydrological seasons and topo-gradient zones, spanning from small CH_4 uptake to ~203 mmol m^{-2} d^{-1}. Soil CH_4 fluxes were similarly dynamic and shifted from maximal CH_4 emission (saturated soil) to uptake (dry soil). In Lower and Transitional zones respectively, tree stem CH_4 contribution to the net ecosystem flux was greatest during flooded conditions (49.9 and 70.2 %) but less important during dry periods (3.1 and 28.2 %). Minor tree stem emissions from the Upper elevation zone still offset the Upper zone CH_4 soil sink capacity by ~51% during dry conditions. Water table height was the strongest driver of tree stem CH_4 fluxes, however tree emissions peaked once the soil was inundated and did not increase with further water depth. This study highlights the importance of quantifying the wetland tree stem CH_4 emissions pathway as an important and seasonally oscillating component of wetland CH_4 budgets.

Plain language summary

Wetland tree stems were recently shown to emit the potent greenhouse gas – methane (CH_4), which is ~45 more powerful than carbon dioxide at warming the Earth's atmosphere. With very few studies ever published on this 'treethane' phenomenon, it is still largely unknown as to why, when and how much methane wetland trees may contribute to the natural emissions from wetland ecosystems. This is important to understand in the context of global methane budgets, climate change and future atmospheric models. Our study measured some of the first-ever wetland tree stem methane emissions spanning an annual cycle, accounting for the seasonal changes in water level of an ephemeral forested wetland - dominated by *Melaleuca quinquenervia* trees. Under the wettest conditions, we found that tree stems emitted the most

methane, and accounted for the majority of the total wetland flux (compared to methane emissions from the wetland water surface). We hypothesize that the methane is largely coming from the low-oxygen wetland soils, and is being transported upwards through the tree roots, transpiration stream and bark layers. The tree stem methane emissions were less important during dry periods, when soil methane emissions were dominant. Overall, tree stems contributed 28-68 % of the annual methane emissions from the wetland forest, highlighting the importance of accounting for tree stem methane emissions within wetland methane budgets.

1.0 Introduction

Methane (CH_4) is a greenhouse gas ~45 times more potent than carbon dioxide, and responsible for about one third of current atmospheric radiative forcing (Masson-Delmotte et al., 2021; Neubauer & Megonigal, 2015). Atmospheric CH_4 concentrations are rising rapidly (Peng et al., 2022; Saunois et al., 2016) and a thorough understanding of all CH_4 sources (both natural and anthropogenic) is important for climate change management and mitigation strategies. Currently, ~60 % of the global annual CH_4 emissions are attributed to anthropogenic sources such as fossil fuel use, transportation and agricultural sectors, whereas tropical wetlands (< 30° latitude) represent the largest natural source of CH_4 (Saunois et al., 2020).

Wetland CH_4 is largely produced within reduced anaerobic soils, then emitted to the atmosphere via ebullition, diffusion and herbaceous plant-mediated pathways (Bartlett & Harriss, 1993; Boon & Sorrell, 1995; Chanton et al., 1989; Jeffrey et al., 2019a). Only recently was woody wetland vegetation (i.e., tree stems) recognized as a potentially important wetland CH_4 source within global wetland CH_4 budgets (Masson-Delmotte et al., 2021; Saunois et al., 2020), but due to a lack of measurements, tree stems are currently not considered as a distinct emission category. The poorly constrained contribution of wetland tree stem CH_4 emissions to the total wetland CH_4 budgets may explain the large discrepancies between bottom-up and top-down estimates, and may also help explain large uncertainties surrounding global wetland CH_4 emissions (Masson-Delmotte et al., 2021; Pangala et al., 2017; Saunois et al., 2020).

Research on tree stem CH_4 emissions has been gaining rapid momentum having recently been coined a '*new frontier of the global carbon cycle*' (Barba et al., 2019a; Covey & Megonigal, 2019). Two-thirds of all tree CH_4 literature was published within the last three years. Tree stem CH_4 emissions have now been reported from various ecosystems including upland forests (Barba et al., 2019b; Machacova et al., 2016; Machacova et al., 2023; Pitz & Megonigal, 2017; Wang et al., 2016), mangrove forests (Gao et al., 2021; Jeffrey et al., 2019b; Zhang et al., 2022), riparian forests (Flanagan et al., 2021; Gauci et al., 2022) and standing deadwood, snags or ghost forests (Carmichael & Smith, 2016; Martinez & Ardon, 2021; Warner et al., 2017). The highest tree stem CH_4 emissions, however, are exclusively attributed to forested wetland ecosystems, also known as lowland forests (Gauci et al., 2010; Jeffrey et al., 2021b; Pangala et al., 2013; Terazawa et al., 2007). For example, in the

Amazon floodplain, tree stem CH_4 emissions were estimated to contribute half of all CH_4 emissions from the Amazonian wetlands (Pangala et al., 2017) and up to 30% of the net ecosystem CH_4 emissions of Panamanian neotropical peatlands (Sjögersten et al., 2020). Similar in magnitude, in subtropical Australian freshwater wetland forests, flooded tree stem CH_4 fluxes were a significant CH_4 source to the atmosphere (Jeffrey et al., 2020a). However, none of these previous studies accounted for bi-monthly-scale variability in CH_4 fluxes over an annual cycle.

The origins and drivers of tree stem CH_4 emissions are complex. Sources of CH_4 have been attributed to a combination of microbial production within wet or rotting heartwood (Wang et al., 2021; Yip et al., 2019; Zeikus & Ward, 1974), saprotrophic fungi (Lenhart et al., 2012) and/or from soil methanogenesis where trees provide a conduit for CH_4 emissions (Jeffrey et al., 2021b). In wetland forests, this is particularly important, as soil CH_4 is transported upwards either passively via diffusion, or actively via plant tissues and the transpiration stream, and eventually egressed via tree stems. Studies on the microbial drivers of tree stem CH_4 have also revealed methanogenic communities living within heartwood and living tissues (Feng et al., 2022; Smits et al., 2021; Yip et al., 2019) and also methanotrophic communities within the phyllosphere i.e. stems, bark and leaves (Feng et al., 2022; Jeffrey et al., 2021a; Putkinen et al., 2021). Thus, it is clear that methane fluxes from trees can come from diverse sources.

The use of natural and labelled isotopic tracers investigating connectivity between the soil - tree stem - atmospheric continuum, have provided compelling evidence for a soil microbial source of tree stem CH_4, due to overlapping isotopic signatures and correlations with soil CH_4 fluxes (Jeffrey et al., 2021b; Megonigal et al., 2019; Pangala et al., 2017; Plain & Epron, 2021). Increased soil moisture (favouring anaerobic soil conditions and methanogenesis) has also been well-documented as a positive driver of wetland tree stem CH_4 fluxes (Jeffrey et al., 2020a; Pangala et al., 2014; Pitz et al., 2018; Terazawa et al., 2021). Furthermore, the typically logarithmic decay in vertical CH_4 emission rates with stem height distance from soil, also suggests a below-ground CH_4 source in wetland forests (Jeffrey et al., 2020b; Sjögersten et al., 2020). Ephemeral forested wetlands undergoing dynamic seasonal and hydrological oscillations in water table height, soil moisture and soil redox potentials are an ideal location to monitor both drivers of wetland tree stem CH_4 emissions and to also document potential seasonal changes in the relative contribution of trees to the net annual wetland CH_4 flux.

Along the east-coast of Australia, many ephemeral wetland forests are dominated by *Melaleuca quinquenervia* (Cav.) S.T. Blake, colloquially known as the 'broad-leaved paperbark'. These forests have a high carbon storage capacity and have recently been incorporated into Australian blue carbon accounting (Lovelock et al., 2022). *M. quinquenervia* generally grow as mono-specific stands and have adapted to withstand brackish to freshwater conditions, acidic soils, heavy clays, moderate bushfires and can tolerate semi-permanent inundation once established (McJannet, 2008). The stems feature a bark that is distinctly unique and comprised of thick, spongy, peeling and paper-like layers (Chiang & Wang, 1984). Due to their hardy and invasive nature, *M. quinquenervia* can readily colonize pasture, and can form dense stands in seasonal wetlands and flooded environments (Johnston et al., 2003). The species has also been introduced to tropical and subtropical lowlands around the world as a fast-growing forestry alternative, promote water table draw-down and/or for exotic aesthetic reasons (CABI, 2023). As such, *M. quinquenervia* are found in at least 57 countries including coastal Asia, the Middle East, Africa and Northern, Central and Southern Americas. Outside of Australia, *M. quinquenervia* is broadly classified as an invasive species, particularly in the Everglades National Park, Florida (USA) where they now occupy ~200,000 ha (Center et al., 2012).

Although *M. quinquenervia* have been previously shown to emit high rates of CH_4 from their stems under flooded conditions (Iram et al., 2022; Jeffrey et al., 2020a; Jeffrey et al., 2020b; Jeffrey et al., 2021b), no study has captured the transitions between inundated and dry conditions to evaluate their contribution tree stem CH_4 emissions to net annual wetland CH_4 budgets. This study aimed to quantify both the annual and seasonal changes to tree stem CH_4 emissions along a forest hydro-topo-gradient and to determine the drivers of tree stem CH_4 fluxes. We hypothesize that *M. quinquenervia* tree stems are a major source of the net wetland CH_4 emissions, and this is related to soil CH_4 production that is moderated by site hydrological conditions.

2.0 METHODS

2.1 Site and elevations

The coastal freshwater wetland investigated here is located near Bogangar in subtropical NSW, Australia (Fig. 1). The site was originally cleared during the 1970's, however by the mid-1980s, fringing trees started to recolonize the site. Within two decades, the wetland

became dominated by a dense monoculture stand of *M. quinquenervia*. The wetland is located within a coastal hind-dune system with soils that are primarily Pleistocene aeolian sands, with a shallow organic-rich surface horizon. During periods of heavy rainfall, surface water within the ephemeral wetland can persist for several months and reach depths of up to ~ 2 m in lower parts of the wetland before completely receding during dry seasons (Fig. 1). The subtropical climate experiences a summer-dominated mean rainfall of 1812 mm per year, with generally dry conditions in winter between July to September (BOM, 2023a).

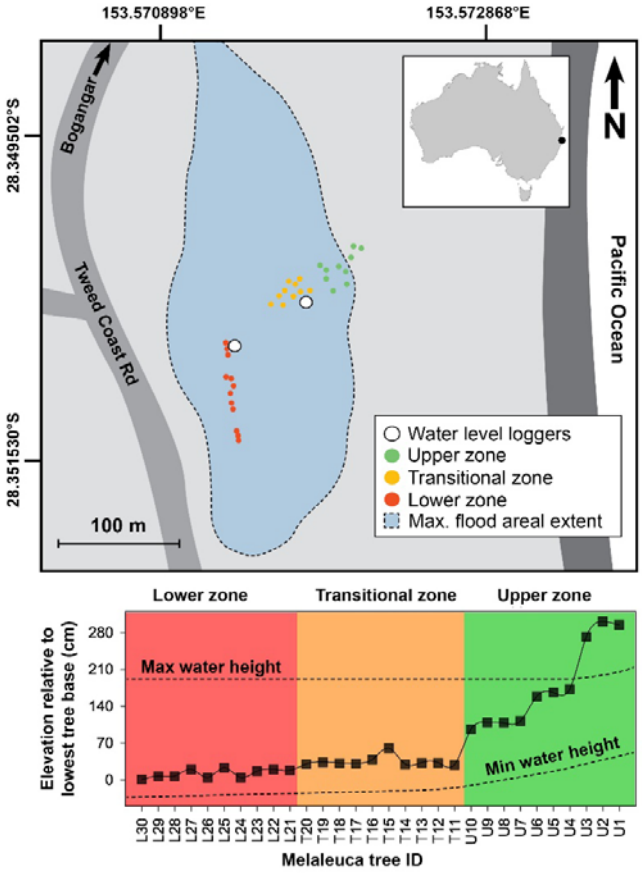

Figure 1. Map of study site in the upper panel showing locations of sampled *Melaleuca* trees (red, yellow and green dots), the location of water level loggers (white dots). The lower panel shows hydro-topological zones and tree base elevational differences relative to the lowest location in the wetland forest (black squares).

Based on a topographic gradient from east to west, our study design split the forest into three distinct hydro-topo-gradient areas, from herein classified as 'Upper', 'Transitional' and 'Lower' zones (Fig. 1). In the Upper zone, *M. quinquenervia* were interspersed with other coastal heath species (*Banksia integrefolia, Casuarina glauca*) and grasses (*Lomandra hysterix*) and generally sit above the soil water logging threshold. Thus, this zone can be considered a largely non-wetland ecotone and used as a comparative control for the wetland forest. The Transitional and Lower zones consisted of a dense monoculture stands of *M. quinquenervia* with no understory vegetation. Within each zone, 10 mature trees of various stem sizes (diameter at breast height (DBH) ranging from 12 to 42 cm) were randomly selected and labelled for the duration of the study. Eight field campaigns were conducted over a 12-month period. Sampling for campaigns 1, 2, 6, 7 and 8 were mostly conducted from a small boat as the water depth in the forest was >1 m. Data analysis were sub-grouped (below) to compare the wetland hydrological campaigns featuring surface waters called 'Wet' (campaigns 1, 2, 6, 7 and 8) vs campaigns featuring exposed soil surfaces called 'Dry' (campaigns 3, 4 and 5).

2.2 Soil and aquatic physicochemical parameters and CH_4 concentrations

During Wet conditions (campaigns 6 and 7), triplicate surface water samples within the forest were measured at various depths for pH, temperature (°C), EC and redox potential (mV) directly from the side of the boat using pre-calibrated multiprobes (HQ40d, Hach). During Dry conditions (campaigns 4 and 5), porewater was collected from various subsurface depths using an extendable push point piezometer (Sonlist), transferred via gas tubing (Bev-A-Line IV).The soil volumetric water content (VWC %) was measured in duplicate at 10 cm soil depth (north and south side) for each tree (Hydro Sense II, Campbell Scientific, detection limit up to 50 % VWC) when the water was below the surface.

To measure dissolved CH_4 concentrations of surface water and porewater, duplicate water samples were collected (as described above) using tubing and 150 mL syringes and from various depths below the water surface (Wet campaigns 6 and 7) or below the soil surface (Dry campaigns 4 and 5). A 40 mL sample of the collected water was equilibrated in the syringe with 110 mL of atmospheric air headspace via vigorous shaking for four minutes (Borges et al., 2015; Roberts & Shiller, 2015). The CH_4 equilibrated headspace was then added to 1 L foil gas bag (Cali-5-bond, Calibrated Instruments) and diluted with 750 mL

atmospheric air. The gas bags (i.e., now containing 900 mL gas sample) were connected to a field portable cavity ring-down spectrometer CH_4 analyzer (CRDS, G4301 Gas Scouter, Picarro) and the mean CH_4 concentration was recorded (ppm). The initial concentrations were then back-calculated as dissolved CH_4 (µM) to account for dilution with ambient air (CH_4 concentration measured *in situ* with the CRDS) and corrected for the temperature-dependant CH_4 solubility coefficient (Wiesenburg & Guinasso Jr, 1979).

2.3 Tree, soil and aquatic CH_4 flux measurements

Tree stem CH_4 fluxes were measured using a 30 cm tall by 40 cm wide semi-rigid wrappable chamber carefully attached to each tree using straps, as described by Siegenthaler et al. (2016). The chamber was connected to the CRDS (listed above) via gas tubing (Bev-A-Line IV) passing through a drying desiccant (Drierite) via a closed loop. The CRDS was factory calibrated and features a precision of ± 0.3 ppb and lower detection limit of 0.9 ppb. During each campaign, CH_4 tree fluxes were measured from four stem heights on 30 individual trees at 10-40 cm, 40-70 cm, 70-100 cm and 100-130 cm above the soil or water level. Once chambers were sealed to the tree stems, the concentration was recorded until a clear linear flux rate was observed for 150 seconds (median value) on high CH_4 fluxing trees and up to 15 minutes on low CH_4 fluxing trees.

Soil CH_4 fluxes were measured during dry campaigns within a 1 m radius of each sampled tree, using a 26 cm diameter x 15 cm high circular PVC chamber, that was first gently inserted ~2 cm into the soil to create a circular groove on the soil surface. The chamber was then immediately removed and flushed with ambient air, before being gently replaced back onto the same soil surface location. Care was taken not to apply downward pressure or step close to the chamber, ensuring no gas efflux enhancement, which was confirmed by real-time observation of the linearity of the fluxes. The fluxes were recorded using similar closed-loop methods and the same CRDS equipment as the tree stem measurements. The soil CH_4 flux was recorded for 300 seconds (median), but up to 14 minutes during low CH_4 fluxing conditions.

Aquatic CH_4 fluxes were measured during flooded wetland campaigns within a 1 m radius of each sampled tree using a 28 cm wide x 25 cm high floating chamber. All measurements were performed from a small boat so as not to disturb the wetland sediments. Any chambers

242 featuring non-linear trends in CH_4 were disregarded and repeated. The flux was measured for
243 300 seconds (median), but as long as 13 minutes during low CH_4 flux measurements.

244

245 **2.4 CH_4 flux calculations and linear flux thresholds**

246 The CH_4 fluxes (F) for trees, soil and water were calculated using the equation:

247 $$F = (s(V/RT_{air}A))t \quad (1)$$

248 where s is the regression slope for each chamber incubation deployment (ppm sec^{-1}), V is the
249 chamber volume (m^3), R is the universal gas constant (8.205 x 10^{-5} $m^3.atm^{-1}.K^{-1}.mol^{-1}$), T_{air} is
250 the mean air temperature recorded inside the chamber in degrees Kelvin (°K), A is the surface
251 area of each chamber (m^2) and t is the conversion factor from seconds to day, and to mmol of
252 CH_4. The s and T_{air} terms were extracted in *R* studio (version 3.5.1) using a modified
253 '*GasFlux'* package of Fuss (2019). The V term (i.e. total volume of the closed loop including
254 chamber, 4 m length of gas tubing, desiccant canister and internal volume of CRDS) was
255 calculated as described by Jeffrey et al. (2020b).

256 Linear flux r^2 value thresholds were dependent upon measurement type and location. Any
257 low r^2 values <0.70 were manually and visually reviewed using the '*GasFlux'* package of
258 Fuss (2019) that generates plots of each individual incubation flux. The average aquatic flux
259 r^2 was 0.96 ± 0.01 (n=85, where ± is SE herein) and the average soil flux r^2 value was 0.95 ±
260 0.01 (n=100). The overall average tree stem CH_4 flux r^2 of 0.88 ± 0.01 (n=890) was lower
261 than the aquatic and soil r^2 values, due to several low CH_4 fluxing upper tree stem
262 measurements and Upper zone trees, particularly during dry campaigns (i.e. trees of slight
263 CH_4 emission or slight uptake). The median r^2 for linear regression of Lower, Transitional
264 and Upper zone tree stem fluxes was 0.99, 0.99 and 0.87, respectively. The simultaneously
265 recorded linear tree stem CO_2 fluxes were used as a proxy for assessing air-tight chamber
266 seals, particularly on low CH_4 fluxing trees. Occasionally, white potting clay was used to fill
267 any gaps between the chambers and tree stems, on trees featuring cracks, fissures, anomalies
268 or splits in the bark.

269

270 **2.5 Up-scaling tree stem CH_4 fluxes**

Individual stem circumferences of the 30 trees were measured during the driest campaign at 10 cm increments from 0 cm (basal area) up to 200 cm stem height above the soil with a tape measure. The forest density (trees ha^{-1}), DBH of all trees (cm) and mean tree height was estimated using a LiDAR enabled smartphone (iPhone 12 Pro, Apple) and forestry scanning app (Arboreal Forest, Arboreal AB). Tree density and size was scanned and calculated within triplicate 50 m^2 plots within each zone.

To upscale the stem CH_4 fluxes measured at various heights into emissions from individual trees, we assumed a simple non-branching tree with a single cylindrical inward tapering stem to a height of 1.3 m above soil or water. During the highest water period, we assumed tree stem circumference did not change above the 2 m high circumference measurement (as mentioned above). The stem surface area was sectioned into radial bands and the CH_4 fluxes at the corresponding band heights were applied and integrated according to Jeffrey et al. (2020b) and similar to Pangala et al. (2017) using the equation:

$$F_t = \int_{0.1}^{1.3} (c.h.F) \quad (2)$$

where F_t is the flux per tree (mmol per tree d^{-1}), c is the tree circumference (m) for each flux measurement location (adjusted for each campaign depending upon the water height above the soil), h is the height (m) for each tree segment (i.e. 30 cm as limited by chamber height) and F is the measured CH_4 flux rate for that height (mmol m^{-2} d^{-1}). The upscaled ecosystem tree stem flux was first calculated using a tree area-weighted flux rate (F_{taw} in mol CH_4 ha^{-1} d^{-1}) for each hydro-topo-gradient zone and during each campaign using:

$$F_{taw} = \bar{x}F_t.d \quad (3)$$

where $\bar{x}$ is the mean and d is the tree density (trees ha^{-1}). Because the mean flux from the selected mature-sized trees may have positively biased the upscaling calculation, a second conservative upscaling approach was compared that accounted for the broad range of tree stem sizes in the forest (range 4.7 – 33.5 cm), as measured in density plots (methods described above). First, the average *M. quinquenervia* bark surface area of tree stems to 1.3 m stem height was estimated by multiplying π by the average DBH (m) of all trees measured within the triplicate forest density plots (Lower zone n=101 trees, Transitional zone n=67 trees, Upper zone n=52 trees) by a height of 1.3 m. This assumes a cylindrical stem shape (i.e. conservative stem area that does not account for larger basal area). This was then

upscaled to estimate bark area (B_a) per hectare (m^2 ha^{-1}) by multiplying by d (as above) for each zone:

$$B_a = d.\bar{x}\text{DBH}.\pi.1.3\text{m} \quad (4)$$

Then for each campaign, the sum of sampled tree emissions per day to 1.3 m stem height (i.e. $\sum F_t$ in eq. 2) within each zone was divided by the $\sum$ of bark surface area to 1.3 m (in m^2) of same trees, thus estimating the average CH_4 flux rate (mmol m^{-2} of bark d^{-1}) from each zone and campaign. This was then multiplied by B_a ha^{-1} (m^2 ha^{-1}) as the second estimate for upscaled tree CH_4 flux (mol ha^{-1} d^{-1}). This approach reduced our tree emissions estimates by an average of 35.7 ± 4.5 % from the first approach (Eq. 3). The soil and aquatic CH_4 fluxes were upscaled by first deducting the tree basal surface area per hectare (m^2 ha^{-1}) from the forest floor from within each hydro-topological zone, then multiplying the remaining soil/aquatic surface area by the average CH_4 flux rate.

For each campaign, the net ecosystem flux from trees (NEF, %) was calculated by dividing the upscaled tree CH_4 flux (mol ha^{-1} d^{-1}) by the sum of CH_4 emissions per hectare (i.e., net tree CH_4 and soil/aquatic flux combined). To estimate the NEF of CH_4 from the wetland over an annual cycle, the results of the eight campaigns were upscaled equally (i.e., 6.5 weeks per campaign). Subsequently, the total CH_4 emission from tree stems (mol ha^{-1} yr^{-1}) was divided by the total CH_4 emission/uptake from soil and water plus the total tree emissions (i.e., the total wetland emissions in mol ha^{-1} yr^{-1}), to determine the NEF from trees (%) over the annual cycle. This was also sub-calculated to specifically compare the contrasting wetland hydrological periods featuring surface waters ('Wet' – campaigns 1, 2, 6, 7, 8) vs exposed soil surfaces ('Dry' – campaigns 3, 4, 5).

2.6 Water table heights and site elevations

The water table was measured *in situ* at two locations (Fig. 1) using a temperature/pressure logger (Diver, Van Essen) recorded at hourly intervals, along with a barometric logger to correct for atmospheric pressure changes over the annual period. The loggers were deployed 1 m below the soil surface within a PVC slotted pipe. During dry campaign, the elevation of each tree relative to the lowest diver logger was surveyed using an optical level (Leica) to correct for the water table vs stem height across the Lower, Transitional and Upper zones.

2.7 Statistical tests

The correlations between two parameters were tested using linear regressions and p values using t-Test: paired two sampling for mean (where $p<0.05$). To test the hypothesis about differences between fluxes from trees within each zone and between wet vs dry conditions, and for soil vs water fluxes within each zone and between wet vs dry conditions,the non-parametric data was analyzed using Kruskal-Wallis one way analysis of variance (ANOVA) on ranks Statistically significant difference was set at $p<0.001$ and was determined using the Dunn's method for multiple pairwise comparisons. Spearman's rank correlation (r_s) coefficients were also used to measure the strength of association between two variables of non-parametric data, for lower tree stem CH_4 fluxes vs VWC (%) and vs soil CH_4 flux.

3.0 Results

3.1 Seasonal rainfall and hydrology

The eight campaigns occurred between June 2021 and May 2022 spanning winter through to the following late autumn and an annual temperature and solar cycle (Fig. 2). This also occurred during two consecutive years of La Niña weather events, characterized by above average rainfall (BOM, 2023b). During the first five campaigns from June 2021 onwards, the wetland water table declined from +48 cm (i.e., above soil surface) to -69 cm (i.e., below the soil surface) within the Lower zone forest. The water table was below ground for campaigns 3-5 during Spring 2021. Summer rainfalls during December 2021 through to February 2022 restored and maintained a shallow standing surface water (~ 20 cm for campaign 6). Two large rainfall events occurring during Autumn in March (351 mm) and April 2022 (343 mm) greatly increased the wetland water table depth, peaking during campaign 7 at 185 cm within the Lower zone forest, 161 cm in the Transitional zone forest and also 18 cm deep in the centre of the Upper zone trees (Figs. 1 & 2).

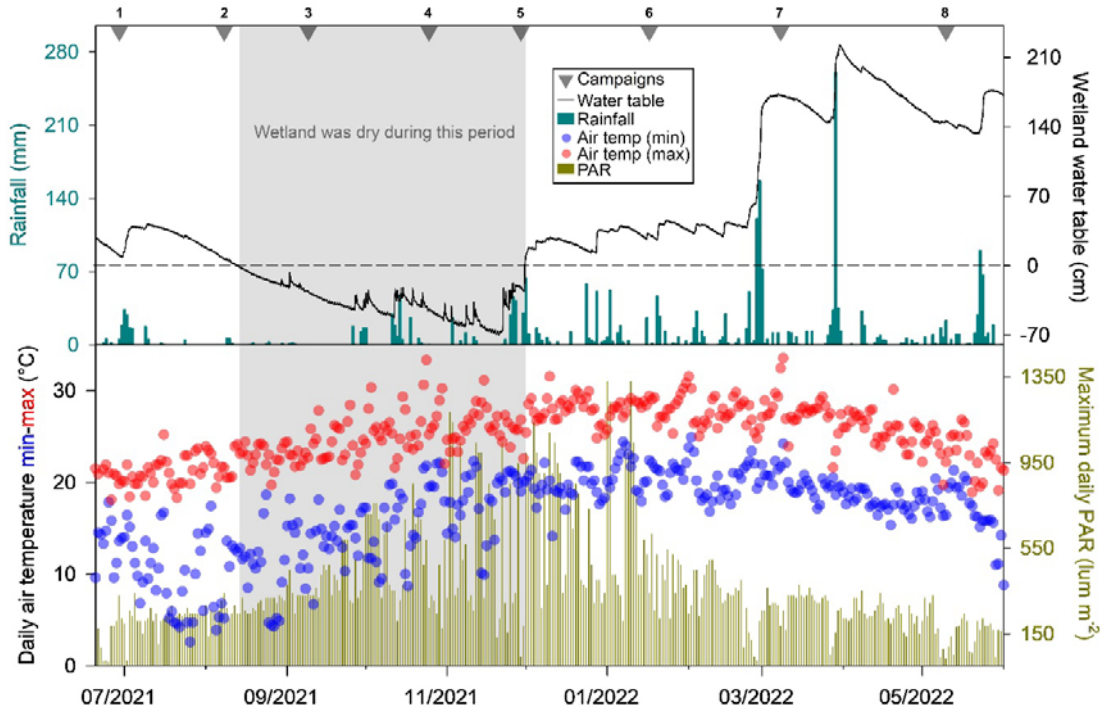

Figure 2. Summary of environmental conditions during the eight study campaigns showing seasonal changes in the Lower zone wetland water table (cm), daily rainfall totals (mm), maximum and minimum air temperature (°C) and photosynthetically available radiation (PAR in lum m^{-2}). Note: Dry campaigns are highlighted in grey.

3.2 Ecosystem parameters, tree size, density and surface area

The sampled *M. quinquenervia* stem diameter at breast height (DBH) ranged from 4.6 – 27.8 cm, 4.7 – 23.8 cm and 5.6 – 33.5 cm from the Lower to Upper zones respectively (Table S1). The average *M. quinquenervia* DBH increased from the Lower to Upper zones and were 11.9 ± 0.6 cm, 12.2 ± 0.7 cm and 15.0 ± 1.0 cm respectively. The average canopy height was 14.1 ± 0.7 m and the tree density was 5049, 4600 and 3466 trees per hectare for the Lower, Transitional and Upper zones respectively (Table S1). Overall, the tree bases only accounted for 2.03 – 2.14 % of the surface area compared to soil/ water surface (i.e., tree base area ha^{-1}).

3.3 Aquatic physicochemical and CH_4 variability

Porewater and surface water CH_4 concentrations (µM) increased with sample depth (Fig. 3, Table S2). The highest porewater CH_4 concentrations were found at -100 cm soil depths

376 which ranged from 54.3 ± 57.7 to 172.2 ± 48.3 µM and shallow porewater CH_4 at -30 cm
377 ranged from 0.33 ± 0.43 to 23.4 ± 12.9 µM. Surface water CH_4 trends were less pronounced
378 vs depth, but CH_4 concentrations were less than porewater and ranged from 2.4 ± 0.02 to 11.0
379 ± 9.7 µM.

380

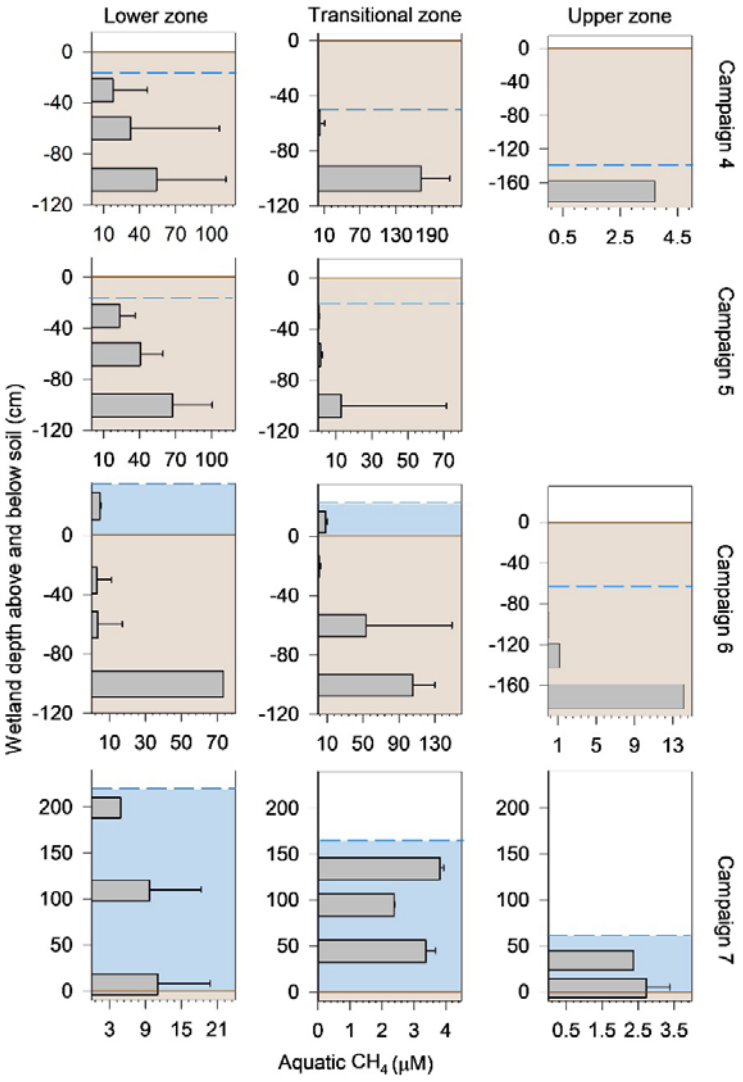

381

382 **Figure 3.** Depth profiles for porewater and surface water CH_4 concentrations (µM) during
383 campaigns 4-7 for each wetland zone. Note: Different x-axis scales used. The brown shaded
384 area represents the soil and blue area is surface water and dashed line is the top of water
385 table. Error bars are SE.

386

3.4 Soil and aquatic CH_4 fluxes

Aquatic CH_4 fluxes were highly variable in the Lower and Transitional zones and the campaign averages ranged from 0.96 ± 0.34 to 5.83 ± 0.72 mmol m^{-2} d^{-1} in the Lower zone, and 0.35 ± 0.10 to 5.36 ± 2.28 mmol m^{-2} d^{-1} in the Transitional zone (Table 1, Fig. 4, Fig. S1). The highest soil fluxes (26.12 ± 34.66 mmol m^{-2} d^{-1}) were observed in the Lower zone when the water table was immediately below the surface during campaign 3. The soil in the Transitional zone was a weak net CH_4 sink during campaign 5 (-0.02 ± 0.01 mmol m^{-2} d^{-1}). The Upper zone soils exhibited slight CH_4 emissions during campaigns 1, 7 and 8 but remained a CH_4 sink for the other five campaigns (Table 1, Fig. 4). There were no significant differences between aquatic CH_4 fluxes between Lower and Transitional zones (p<0.05, Table S3, Fig. S2). There were significant differences between soil and aquatic CH_4 fluxes in the Lower zone between each campaign but not in the Upper zone, and there were significant differences between Lower and Upper zones for both soil and aquatic fluxes (Table S3, Fig. S2).

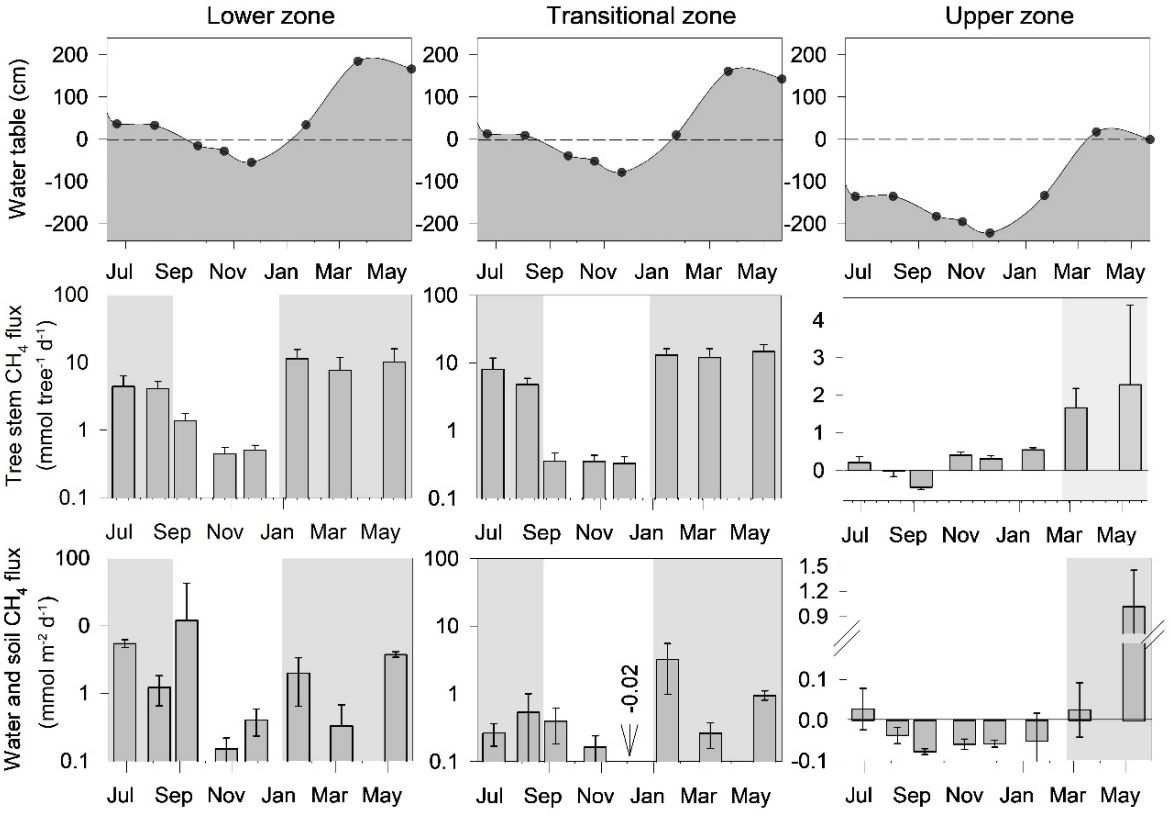

Figure 4. Stacked plots indicating the changing water table within each zone, average CH_4 flux per tree (mmol $tree^{-1}$ d^{-1}) and average CH_4 flux from water or soil (mmol m^{-2} d^{-1}). Note: Different y-axis scales, shaded campaigns are where surface water was present, the horizontal dashed line is soil surface, the horizontal solid line separates CH_4 sink and source in Upper zone. Error bars are SE.

Table 1. Summary of water table (WT), CH_4 fluxes from trees, soil and water surfaces for each zone. Note: all tree fluxes scaled to only 1.3 m of tree stem.

			***Melaleuca* tree stem CH_4 flux**			**Water/Soil CH_4 flux**	
Zone	Trip	WT mean (cm)	(mmol m^{-2} of bark d^{-1})	(mmol $tree^{-1}$ d^{-1})	(mol ha^{-1} d^{-1})	(mmol m^{-2} d^{-1})	(mol ha^{-1} d^{-1})
Lower	1	36.8	7.59	4.48±1.85	18.54	5.83 ±0.72	57.10
	2	33.2	6.79	4.14±1.05	16.60	1.79 ±0.59	17.49
	3	-14.9	2.13	1.40±0.37	5.21	26.12 ±34.66	255.66
	4	-27.7	0.62	0.45±0.10	1.52	0.15 ±0.07	1.49
	5	-54.2	0.63	0.51±0.08	1.55	0.41 ±0.18	4.01
	6	34.4	20.31	11.49±3.98	49.63	3.01 ±1.35	29.41
	7	184.7	13.75	7.74±4.03	33.62	0.96 ±0.34	9.40
	8	166.4	13.25	10.24±5.51	32.39	3.91 ±0.36	38.23
	Wet	91.1	12.34	7.62±3.28	30.15	3.10 ±0.67	30.33
	Dry	-32.3	1.13	0.79±0.18	2.76	8.90 ±11.64	87.05
	Average	**44.8**	**8.13**	**5.06±2.12**	**19.88**	**5.27 ±4.78**	**51.60**
Transitional	1	13.1	9.32	8.18±3.60	21.41	0.35 ±0.10	3.46
	2	9.6	7.62	4.87±1.05	17.49	1.10 ±0.46	10.76
	3	-38.6	0.55	0.36±0.11	1.27	0.72 ±0.22	7.08
	4	-51.4	0.54	0.36±0.08	1.24	0.23 ±0.07	2.28
	5	-77.8	0.48	0.34±0.07	1.10	-0.02 ±0.01	-0.17
	6	10.8	20.38	13.27±3.00	46.79	5.36 ±2.28	52.51
	7	161.0	19.73	12.21±4.00	45.31	0.36 ±0.11	3.48
	8	142.8	25.30	15.03±3.64	58.10	1.02 ±0.15	9.97
	Wet	67.4	16.47	10.71±3.06	37.82	1.64 ±0.62	16.04
	Dry	-55.9	0.52	0.35±0.09	1.20	0.31 ±0.10	3.06
	Average	**21.2**	**10.49**	**6.83±1.94**	**24.09**	**1.14 ±0.42**	**11.17**
Upper	1	-134.8	0.14	0.21±0.16	0.29	0.03 ±0.05	0.27
	2	-134.3	-0.01	-0.01±0.15	-0.03	-0.04 ±0.02	-0.37

3	-181.8	-0.47	-0.45±0.06	-0.99	-0.08 ±0.01	-0.76
4	-194.6	0.51	0.40±0.09	1.07	-0.06 ±0.01	-0.58
5	-221.0	0.26	0.31±0.09	0.55	-0.06 ±0.01	-0.57
6	-132.4	0.61	0.55±0.06	1.29	-0.06 ±0.08	-0.61
7	17.8	2.51	1.67±0.51	5.33	0.03 ±0.07	0.25
8	-0.45	5.12	2.28±2.12	10.84	1.02 ±0.43	10.00
Wet	-76.8	1.67	0.94±0.60	3.54	0.19 ±0.13	1.91
Dry	-199.1	0.10	0.09±0.08	0.21	-0.06 ±0.01	-0.63
Average	**-122.7**	**1.08**	**0.62±0.41**	**2.30**	**0.10 ±0.09**	**0.96**

3.5 Tree stem CH_4 fluxes

Tree stem CH_4 flux rates varied greatly between trees, stem heights, hydrological conditions, campaigns and topography, and ranged from CH_4 uptake to CH_4 fluxes of 203.1 mmol m^{-2} d^{-1}, spanning several orders of magnitude (n=890, Table 1, Fig. S3). The largest tree stem CH_4 fluxes occurred during Wet campaigns and occurred within the Transitional and Lower zones. The highest tree stem CH_4 fluxes were almost always from the lower stem measurement heights (Fig. 5). Tree stems fluxes between Wet and Dry campaigns and within each zone were significantly different (p<0.05, Table S4, Fig. S2). There were no obvious patterns suggesting that the same trees always emitted the highest or lowest fluxes (Fig. S3). A large proportion of the Upper zone tree stems exhibited CH_4 uptake (31% of all measurements, n=81 of 180) during the dry campaigns. Importantly, during Dry campaigns 4 and 5, the tree stem CH_4 fluxes (mmol per tree d^{-1}) were of the same order of magnitude between all site locations (and not significantly different between Lower and Upper zone trees (Table S4, Fig. S3), but were two orders of magnitude different during the during Wet campaigns.

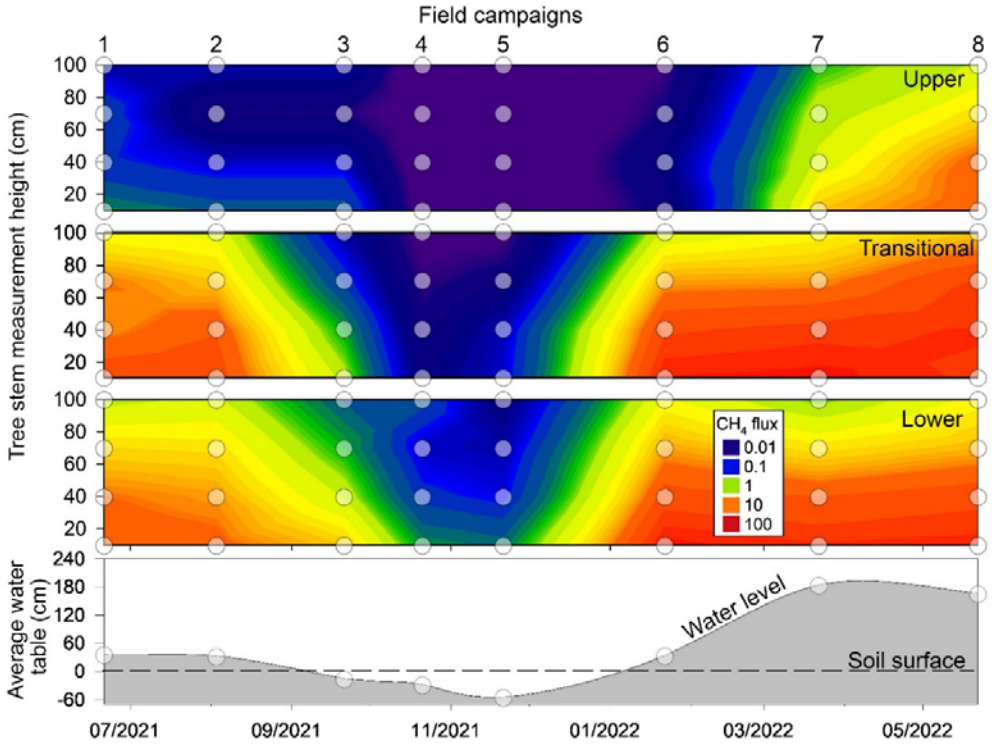

Figure 5. Contour plots showing average tree stem CH_4 flux rates (mmol m^{-2} d^{-1}) at each stem height, from each campaign and within each hydro-topographic zone. Note: log scale of CH_4 flux rates (mmol m^{-2} d^{-1}) and water table is from the Lower zone and the dashed line is the soil surface.

3.6 Drivers of CH_4 fluxes

There were significant negative trends between both porewater CH_4 (µM) vs the porewater redox potential (SHE) (r^2=0.21, p<0.001, n=21) and between dissolved CH_4 vs water table depth (r^2=0.22, p<0.05, n=31) (Fig. S4). There were no apparent trends between porewater CH_4 (µM) at the same depth interval and tree stem fluxes (Fig. S5). During campaigns 3-5, there were significant positive trends between adjacent surface soil moisture (% VWC) and tree stem CH_4 fluxes, (r^2=0.36, p<0.001, n=90) (Fig. 6). During dry conditions, there was also a significant positive relationship between the soil CH_4 fluxes vs lower tree stem CH_4 fluxes (r^2=0.53, p<0.001, n=61) (Fig. 7a). However, during inundated conditions, there was no correlation between tree CH_4 flux vs aquatic CH_4 flux (Fig. 7b). In the Upper zone, there were no trends between either soil moisture and soil CH_4 flux, vs tree stem CH_4 flux.

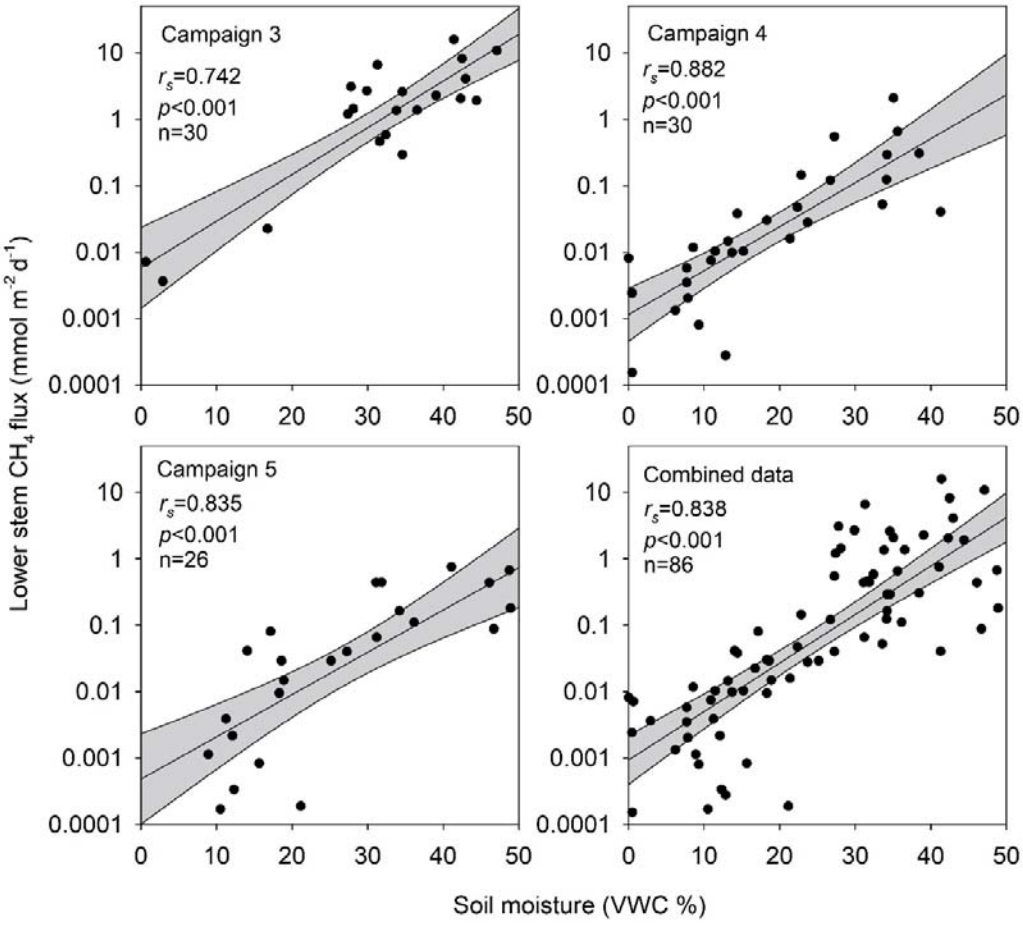

444

445 **Figure 6.** Positive significant correlations between soil WVC% and lower (10-40 cm) tree
446 stem CH_4 fluxes during the three Dry campaigns. Note: log scale y-axis, Spearman's Rho
447 (r_s), grey areas show 99 % confidence interval and 50% VWC is the upper volumetric water
448 content range of the probe.

449

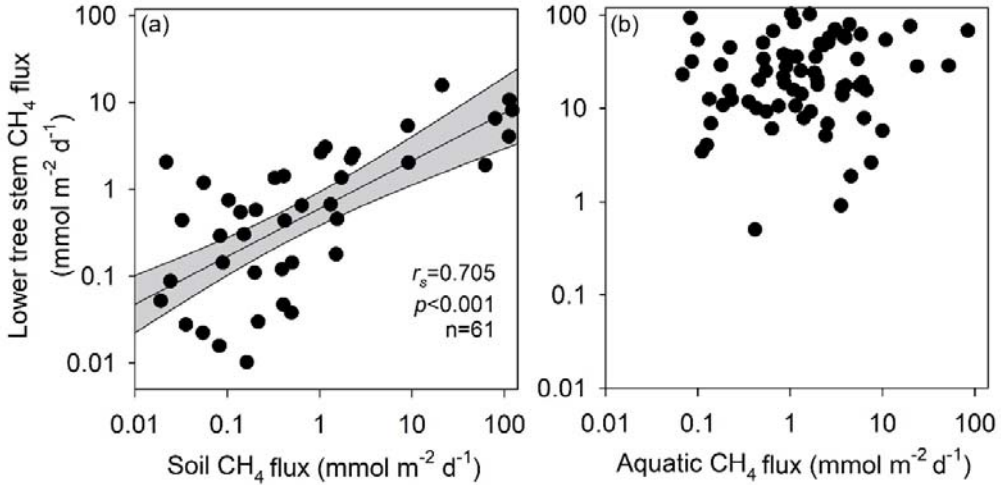

450

451 **Figure 7.** Correlations between lower (10-40 cm) tree stem CH_4 fluxes and a) soil CH_4 fluxes
452 (Dry campaigns) and b) aquatic CH_4 fluxes (Wet campaigns) within the Lower and
453 Transitional hydro-topological zones. Note: Spearman's Rho (r_s) and grey areas show 99 %
454 confidence interval.

455

456 When combining all data in the study, there were no apparent trends between tree stem CH_4
457 flux vs stem height above the soil (Fig. S6). However, when Wet and Dry data campaigns
458 were separated, a positive significant logarithmic trend was observed between Dry campaign
459 tree stem CH_4 flux in relation to the distance to the below-ground water table (r^2=0.55,
460 p<0.005, n=369, Fig. 8a). No trend with the distance above soil height during Wet campaigns
461 was found (Fig 8b), but a decrease in CH_4 flux vs stem height > water was observed (Fig.
462 8b).

463

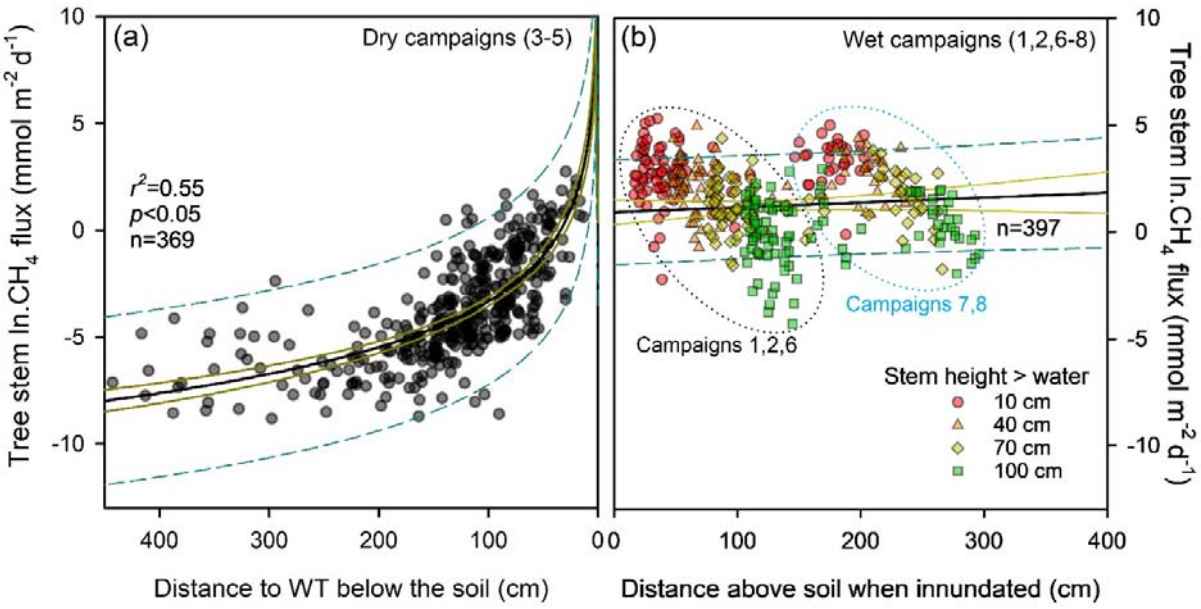

464

465 **Figure 8.** Correlations for all positive tree stem CH_4 flux data vs **(a)** chamber height distance
466 from water table during Dry campaigns, and **(b)** chamber heights above soil surface during
467 Wet campaigns. Note: Log transformed data on y-axis. Yellow lines are 95 % confidence
468 intervals and dashed lines are 95 % prediction intervals.

469

470 **3.7 The net ecosystem flux (NEF) of CH_4 from tree stems**

471 The role of tree stem CH_4 fluxes to the total wetland NEF varied greatly during the study. In
472 the Lower and Transitional zones, the tree stem CH_4 fluxes were substantial contributors to
473 the NEF, particularly during Wet conditions (Fig. 9). The contribution of tree stems to the
474 NEF ranged from 25-93 % during Wet campaigns and were > 6 times higher emitters per
475 hectare than the soil uptake rate during the Dry campaigns. During campaign 3 in the Lower
476 zone, an anomalously large soil CH_4 release occurred when the water table was very near at
477 the soil surface and hence the soil CH_4 flux pathway was the largest contributor to the Lower
478 zone CH_4 emissions during this campaign (Fig. 9).

479 In the Upper zone, tree stem fluxes were minimal yet somewhat dynamic, as tree emissions
480 offset a portion of the soil CH_4 uptake during campaigns 2, 4 and 6, and tree emissions were
481 equal to soil uptake in campaign 5. During campaign 3, the tree stem CH_4 uptake further
482 enhanced the soil CH_4 sink by ~31 %. During the wettest conditions (Campaigns 1, 7 and 8),

the Upper zone trees were the dominant CH_4 emission pathway ranging from 52-96 % of the NEF (Fig. 9).

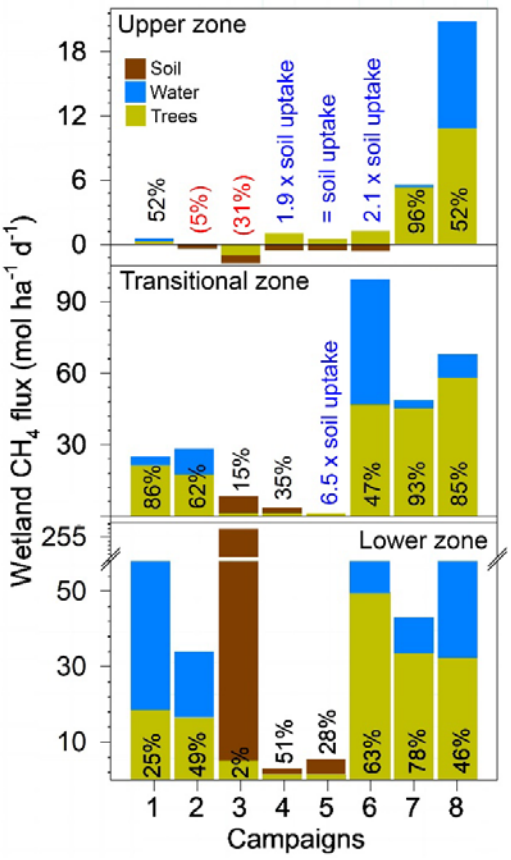

Figure 9. Upscaled wetland CH_4 NEF differentiating the CH_4 flux from tree stems, water and soils from each hydro-topological zone and campaign (mol ha^{-1} d^{-1}). The values above bar plots indicate the tree CH_4 contribution to: (1) the NEF % (black text); (2) offsetting soil CH_4 uptake (blue text), and (3) enhancing soil uptake (red text). Note: different y-axis scales.

4.0 Discussion

4.1 Large variability in tree stem CH_4 emissions

There were significant differences between the tree stem CH_4 fluxes, both between the Wet and Dry seasons, and along the hydro-topo-gradient. The tree stem CH_4 emissions varied by more than six orders of magnitude, ranging from slight CH_4 uptake in the Upper zones during dry conditions, to large CH_4 fluxes up to 203.1 mmol m^{-2} d^{-1} during flooded conditions

(Table 1). Tree stem CH_4 fluxes also varied greatly depending upon which location of the wetland they were measured in, the hydrological conditions under which they were measured and the height on the tree stem at which the fluxes were measured (Fig. 8b).

The largest tree stem CH_4 emissions always occurred during Wet campaigns where the wetland soils were completely inundated in the Lower and Transitional zones (Table 1) and generally from the lowest measurement location on each tree stem (Fig. 5). During periods of flooding, the saturated soils and/or internal tree stem tissues would likely be anaerobic, promoting conditions more suitable for soil and/or internal tree stem methanogenesis to occur, with very little opportunity for aerobic methanotrophy. The lower stem locations are also in closest proximity to any potential soil and porewater CH_4 sources (Jeffrey et al., 2021b; Megonigal et al., 2019). Under these conditions, the saturated bark and tree stems can act like a preferential conduit between the soil and the atmosphere, assisting soil-derived CH_4 in bypassing CH_4 oxidation processes in either the wetland water column or under-lying soil column.

In the Lower and Transitional zones, we found that on average, 56 ± 2.0 % of the total tree stem CH_4 emissions came from the 10-40 cm of stem height measurements, and 83 ± 1.3 % from 10-70 cm of the stem height (Table S5). Interestingly, this ratio did not change between Wet and Dry campaigns (Table S5). The incremental reduction in tree stem CH_4 emissions versus tree stem heights (Fig. 5, 8b) are likely due to a combination of CH_4 being degassed to the atmosphere via the bark during the upwards transport of soil derived CH_4, and losses from bark-dwelling CH_4 oxidizing bacteria (MOB) (Jeffrey et al., 2021a). Although CH_4 oxidation rates by bark-dwelling MOB were not quantified during this study, our previous work using various isotopic and MOB inhibitor approaches, estimated CH_4 oxidation rates of ~33 to 36 % in these same wetland tree species (Jeffrey et al., 2021a; Jeffrey et al., 2021b).

The smallest tree stem CH_4 emissions and sometimes CH_4 uptake, occurred within the Upper zone trees, during the driest conditions and mainly from the upper stem heights (Table 1, Fig. 5). As mentioned above, the CH_4 uptake measured on the tree stems is likely due to the presence of bark-dwelling MOB. The low rates of tree stem CH_4 emission from the Upper zone trees are also likely due to the far deeper water table 1-2 m below the soil surface (Fig. 4). These more ‘upland forest’ soil conditions are generally unsuitable for significant soil methanogenesis to occur and create conditions favourable for the oxidation of deeper groundwater and soil CH_4, prior to entering the tree stems and soil surface.

If the bark-associated methanotrophy and oxidation rates throughout all campaigns are similar to our two previous estimates in *M. quinquenervia* forests (Jeffrey et al., 2021a; Jeffrey et al., 2021b), the large CH_4 emissions reported in the Lower and Transitional zones for this study would likely be substantially greater, if not for bark-dwelling methanotrophic communities mitigating a proportion of the CH_4 egress from the wetland trees. This suggests that whilst *M. quinquenervia* can emit significant quantities CH_4 via their stems, they may also help attenuate soil CH_4 by creating a suitable microbial habitat for methanotrophy (and potentially other microbial metabolic processes) to occur (Bringel & Couée, 2015; Van Stan et al., 2021). Seasonal measurements of bark-associated methanotrophy, however would be required to better constrain this process.

4.2 Dynamic wetland CH_4 emissions from soil and aquatic surfaces

The patterns of the wetland soil and aquatic CH_4 emissions were highly dynamic, but generally concomitant with the water table depth. For example, the highest CH_4 fluxes from the wetland occurred when the soils were inundated, whilst the lowest CH_4 emissions and CH_4 uptake occurred when the water table receded deep below the soil surface (Fig. 4, Fig. S2). This pattern with the water table depth was evident in the Upper zone soils that were a net CH_4 sink during five of the eight campaigns (Fig. 4). This is common for upland forest soils, which are recognized as the largest biological sink for atmospheric CH_4 due to soil associated methanotrophy (Kirschke et al., 2013; Saunois et al., 2020).

In the Lower zone, even during the driest campaigns, the wetland soil always remained a net CH_4 source as the water table was never lower than ~55 cm below the soil surface. During campaign three, a large soil CH_4 release was observed when the water table was within ≤ 14 cm of the soil surface, but was generally water-logged around the base of most trees (Figs. 4, 9). During this time, the water table had just receded after several months of inundation and the Lower soils were still highly saturated leading to a likely low redox potential (as indicated by soil moisture content (%) near or greater than 50 %, Fig. 6). Under these conditions, there is little potential for aerobic soil CH_4 oxidation to occur, and this most likely explains the highest rates soil CH_4 fluxes reported in this study (26.1 mmol m^{-2} d^{-1}). Although the soil CH_4 flux rates during campaign 3 greatly skewed the annual soil CH_4 emission estimates for the Lower zone (Table 1), we do not consider these as outliers (Fig. S2) as they likely

captured a genuine temporal "hot spot" and pulse release of soil CH_4. Observations such as this short-term pulse serve to reinforce the importance of temporal monitoring CH_4 fluxes from natural ecosystems undergoing dynamic hydrological oscillations and changing redox conditions, where significant episodic emissions can take place over short timescales.

Although the Transitional zone soil and aquatic surfaces were net CH_4 sources over the annual cycle, once the water table dropped to ~75 cm below the soil surface (Campaign 5, Fig 4), the Transitional zone soils switched to a net CH_4 sink (Fig. 4). This soil CH_4 sink occurred despite the Transitional zone tree stems continuing to emit CH_4 (Fig. 4). Importantly, at this time, the tree stem fluxes (1.1 mol ha^{-1} d^{-1}) offset the adjacent soil uptake (-0.17 mol ha^{-1} d^{-1}) by ~6.5 times (Fig. 9, Table 1). This suggests that somewhere between these two water table depths (-55 cm in Lower zone as mentioned above, and -75 cm in the Transitional zone), soil-associated methanotrophy may completely oxidize CH_4 during upward transport through the soil column before CH_4 can escape to the atmosphere (Barbosa et al., 2018). This depth is likely to be influenced by soil type and is therefore site dependent. In our case, it also shows that soil-derived CH_4 can effectively bypass soil CH_4 oxidation if transported via the tree stems to the atmosphere.

The dynamic range in CH_4 flux and intra-site variability highlights the importance of measuring wetland tree stem CH_4 fluxes along hydro-topo-gradients, whilst capturing multiple tree stem heights and over multiple campaigns to accurately constrain the annual contributions of tree stem fluxes to forested wetland CH_4 budgets. This study also captured a large variability in the CH_4 fluxes from each tree within each zone, reiterating the importance of replicate measurements.

4.3 Drivers of tree stem CH_4 emissions

Trends with upland forest tree stem CH_4 emissions and soil CH_4 can be complex, as trees can act as CH_4 sources, whilst the well aerated soils represent net CH_4 sinks (Barba et al., 2019b; Machacova et al., 2023; Wang et al., 2016). Within the Upper zone stand, during most of the campaigns, the drivers were also unclear, with the tree stem CH_4 fluxes often shifting between slight CH_4 sources and sinks, between various stem heights and campaigns (Figs. 4,9, Table 1). As such, no clear trends were found with adjacent soil moisture, soil fluxes (mostly uptake) or water table height. Therefore, the Upper zone drivers of CH_4 flux likely

592 differ and/or the smaller signal is masked by higher noise – when compared to wetland trees
593 in the Lower and Transitional zones. Several explanations for upland tree stem CH_4
594 emissions may include: 1) internal heartwood rot and stem moisture niches occupied by
595 methanogens (Feng et al., 2022; Yip et al., 2019); (2) termite-associated CH_4 emissions
596 (Carmichael et al., 2014); (3) CH_4 production by saprotrophic fungi (Lenhart et al., 2012);
597 and/or (4) the transpiration of dissolved CH_4 from deeper groundwater sources from below
598 our measurement locations (Barba et al., 2019a; Covey & Megonigal, 2019).

599 Drivers were clearer in the Lower and Transitional zones, where we found positive
600 significant correlations between tree stem CH_4 fluxes, and both soil moisture content and soil
601 CH_4 fluxes (Figs. 6, 7). These soils were also the locations of the highest porewater CH_4
602 concentrations (Fig. 3) and were inundated for the longest time periods over the study period
603 (Fig. 1). This suggests that soil moisture, reducing soil conditions and high porewater CH_4
604 concentrations (Fig. S4) were the major drivers of tree stem CH_4 emissions. This agrees with
605 previous studies showing similar trends along soil moisture gradients (Daniel et al., 2023;
606 Jeffrey et al., 2020a; Moldaschl et al., 2021; Pitz et al., 2018), via artificial flooding events
607 (Pangala et al., 2014; Terazawa et al., 2021) and with seasonal changes in the forest water
608 table heights (Gauci et al., 2022; Sjögersten et al., 2020). In the same *M. quinquenervia* forest
609 as our present study ~two years prior, the soil and tree stem $\delta^{13}C$-CH_4 (‰) isotopic
610 signatures were shown to overlap (Jeffrey et al., 2021b), further suggesting that most *M.*
611 *quinquenervia* tree stem CH_4 egress originates from the soil methanogenesis zone.

612 In the Lower and Transitional zones, a strong correlation between soil and tree stem CH_4 flux
613 was observed (Fig. 7a), however, no relationship was found between aquatic CH_4 flux and
614 tree stem CH_4 flux (Fig. 7b). If indeed the soil methanogenesis zone was the major driver of
615 tree stem CH_4, we would anticipate a correlation between soil wetted area (i.e., the total
616 methanogenesis zone in the rhizosphere below the soil surface) and the volume of tree roots
617 and tree stem embedded within this zone. For example, with a low water table, a smaller
618 proportion of tree roots would sit within the saturated methanogenesis zone (compared to a
619 high-water table), whilst CH_4 oxidation within the upper rhizosphere would be greatest,
620 and/or the pathway from the soil methanogenesis zone to the tree stem would be longest.
621 Under a scenario of complete inundation (i.e., water table at or above the surface), all of the
622 tree roots would be in the saturated soil methanogenesis zone, and there would be a much
623 shorter pathway for root-entrained CH_4 to tree stem CH_4 egress, as well as decreased CH_4
624 oxidation potential in the rhizosphere. Such a trend was observed when plotting lower tree

stem CH_4 fluxes of the Lower and Transition zones vs the water table height (Fig. 10). The regression in Fig. 10 estimates that for every 30 cm of water table increase below the ground surface (i.e., Dry campaigns), the lower stem tree CH_4 flux rates increased by approximately an order of magnitude, up to a maximum of ~0.27 mmol m^{-2} d^{-1} when the water table was at the surface (Fig. 10). Interestingly, once the water table exceeded the soil surface (Wet campaigns), the tree stem CH_4 flux rates did not continue to rise and reached a CH_4 egress maxima. This process was first proposed by Gauci et al. (2022), who found a remarkedly similar trend in tree stem CH_4 fluxes within an Amazon riparian forest subject to ~12 m amplitude fluctuations in the water table height. Overall, this shows a significant correlation between the depth of the water table below-ground and the root-entrained CH_4 tree stem emissions, whereas tree CH_4 fluxes essentially become de-coupled from the water table dynamics when water levels are above the soil surface (Fig. 10).

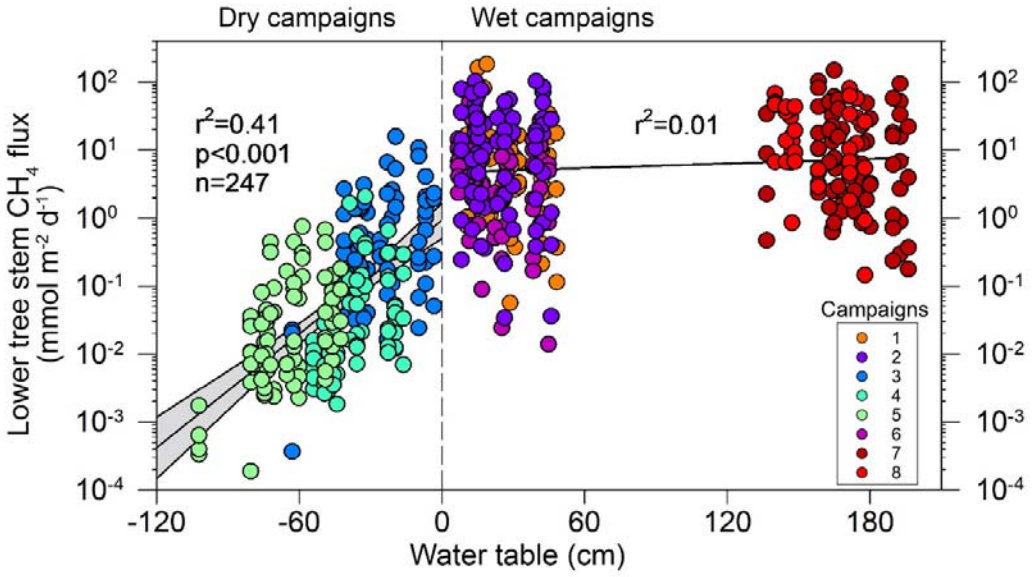

Figure 10. Regression of lower stem tree stem fluxes (10 and 40 cm) vs water table height below the soil surface (Dry campaigns) and above the soil surface (Wet campaigns). Note: Log scale and data for Lower and Transitional zones only. The grey shaded area is the 99 % confidence interval.

4.4 The role of tree stem emissions in the net ecosystem flux (NEF)

The importance of tree stem CH_4 fluxes to the total wetland CH_4 flux or NEF (%) was highly variable and dynamic over the annual cycle. During the Dry campaigns, although soils were the most important pathway for CH_4 emissions, the wetland trees still contributed ~3 to 28 % of CH_4 emissions for the Lower and Transitional zones respectively (Fig. 11). As mentioned previously, a large soil pulse release of CH_4 in the Lower zone (Campaign 3) greatly skewed these upscaled CH_4 emissions and NEF estimates. During Dry conditions in the Upper zone, tree stem emissions were 13-fold lower than Lower zone, however, the tree stems accounted for 100% of the Upper zone NEF as Upper soils were a net CH_4 sink (-0.06 mmol m^{-2} d^{-1}, Table 1). This is important to consider in future upland forest CH_4 budgets which are conventionally considered as net CH_4 sinks.

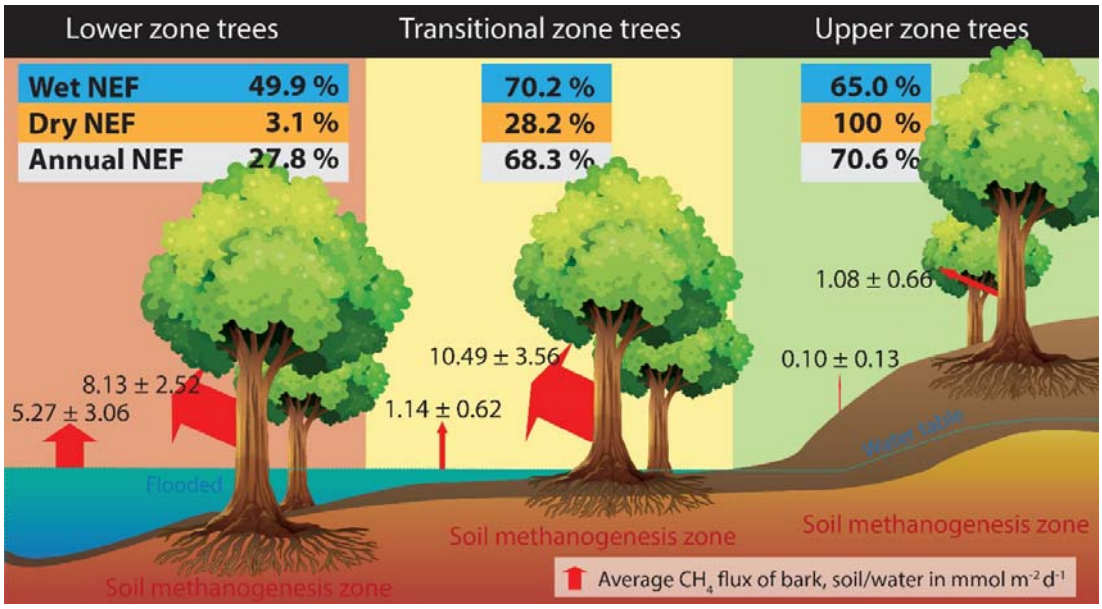

Figure 11. Conceptual summary diagram of the net ecosystem CH_4 flux from trees (NEF, %) during Wet campaigns (n=5), Dry campaigns (n=3) and annual emissions (n=8). The average CH_4 flux rates for each pathway (mmol m^{-2} d^{-1}) are shown with arrow size depicting the scale of emissions.

During Wet campaigns, tree stem CH_4 fluxes were equal to, and the most important pathway, of the total wetland efflux, accounting for 50-70 % of the NEF of the Lower and Transitional zones respectively (Figs. 9, 11). This is similar to the range of estimates for other lowland forest studies, including ~50 % of the NEF in flooded forests of the Amazon basin (Pangala

et al., 2017), 62-87 % in tropical wetlands (Pangala et al., 2013) and 30 % in neotropical peatland forest (Sjögersten et al., 2020). It should be noted that we did not account for the aquatic CH_4 ebullition pathway in our study design, though very little ebullition was observed from the sandy sediments during inundated campaigns. However, in some wetland systems, ebullition can represent a major component of wetland CH_4 budgets (Aben et al., 2017; DelSontro et al., 2016; Jeffrey et al., 2019a).

To the best of our knowledge, no other studies have captured forested wetland CH_4 emissions at monthly/bi-monthly sampling temporal resolution over an annual cycle. During the entire study, we calculate that the subtropical *M. quinquenervia* tree stems contributed ~27.8 – 68.3 % of the NEF from the Lower and Transitional zones of the wetland respectively (Fig. 11). This study provides clear evidence that tree stems are a significant and often missing component of many previous wetland CH_4 budgets, where they have been largely overlooked (Barba et al., 2019a; Covey & Megonigal, 2019). The CH_4 flux rates and upscaled rates from the subtropical *M. quinquenervia* trees (per hectare) were at the upper range of other reported tree stem fluxes from the literature (Fig. 12). Generally, the lowest ecosystem tree CH_4 emissions per hectare come from temperate upland forests and mangrove forests, whereas peatland and wetland forests can be up to five orders of magnitude higher (Fig.12). Our upscaled results (1187 to 37,803 mmol ha^{-1} d^{-1}) were higher, yet similar in range, to the tropical flooded forests of the Amazon (2937 to 28,493 mmol ha^{-1} d^{-1}; Pangala et al., 2017) and neotropical peatland (2999 to 21,745 mmol ha^{-1} d^{-1}; Sjögersten et al., 2020) (Fig. 12), higher than seasonally flooded tropical forest in French Guiana (-101 to 183 mmol ha^{-1} d^{-1}; Daniel et al., 2023) and tropical SE Asian peat forest (419 to 1878 mmol ha^{-1} d^{-1}; Pangala et al., 2013).

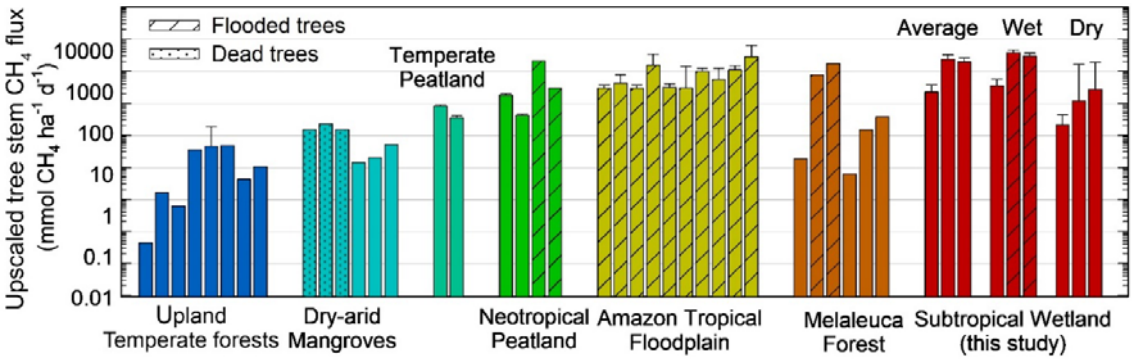

Figure 12. Comparison of previously reported tree stem ecosystem CH4 flux rates spanning various forest types (Covey & Megonigal, 2019; Jeffrey et al., 2020a; Jeffrey et al., 2019b; Sjögersten et al., 2020) compared to the average, Wet and Dry tree CH4 emissions of our study. Note: The log scale on the y-axis.

It is important to note that the up-scaling approach used can greatly influence the interpretation of results, both here and for future studies. For example, if using Eq. 3 for upscaling (i.e., the average CH_4 flux per tree multiplied by forest density – a common upscaling approach), our upscaled tree stem CH_4 emissions per hectare would have been on average ~ 35.7 ± 4.5 % greater than we reported. The approach we applied here considers the individual surface areas of all tree stems per hectare (i.e., integrating Eq. 4) and integrates this into the upscaling to ecosystem level. This approach is likely more realistic as we better account for the large variability in stem sizes of the dense stands of *M. quinquenervia*. This approach may be less important in forests and stands featuring more uniformity in tree size. Furthermore, we did not account for any tree stem CH_4 emissions below a 10 cm stem height (near the location of highest CH_4 emissions, Table S5). For example, the lower 30 cm of stem was previously shown to account for > 90 % of stem CH_4 efflux in *M. quinquenervia* forest (Jeffrey et al., 2020b). We also did not account for multiple trunked or branched tree stems (i.e., we only measured and/or counted all as single stems). We also did not project any CH_4 emissions beyond the 130 cm stem height that were measured – therefore, our upscaled results should be considered as a conservative estimate.

4.5 Conclusion and future directions

Overall, our study highlights the significant role of trees, and the importance of accounting for tree stem CH_4 emissions from (sub)tropical forested wetlands, to better estimate total wetland CH_4 budgets. We also highlighted the extremely large range in tree stem CH_4 flux variability both within a site, across seasons and at individual tree stem heights. Tree stem CH_4 emissions appear to be mainly driven by water table height, which moderated the soil methanogenesis zone and porewater redox potentials. The CH_4 flux rates and upscaled emissions from *M. quinquenervia* forests presented here are at the higher end of reported literature values. This may be due to the wetland soil carbon and waterlogging conditions, (sub)tropical climate driving microbial metabolism, tree species-specific physiological

adaptations (including the unique layered bark structure allowing for rapid CH_4 transport from the soils to the atmosphere), and/or high forest density (up to 5049 trees ha^{-1}) typical of *M. quinquenervia* stands. This study also provides important baseline readings for the southern hemisphere and Australian wetland forests, which typically experience highly dynamic rainfall and large soil redox oscillations between flooding and drought conditions.

Future research in forested wetlands should consider all atmospheric pathways for CH_4 by including aquatic ebullition and the importance of episodic pulses of emissions under ideal conditions for methanogenesis. To account for diurnal variability in *M. quinquenervia* tree CH_4 emissions (Jeffrey et al., 2020a; Jeffrey et al., 2021b), which were not measured during this study, future studies should also consider auto-sampler approaches to tree stem CH_4 flux measurements capturing high resolution temporal variability (Barba et al., 2019b; Brechet et al., 2021; Sakabe et al., 2021). Lastly the role of upper stems and branches (recently shown to emit CH_4 in certain upland trees) (Gorgolewski et al., 2022), phyllosphere microbial CH_4 oxidation (Putkinen et al., 2021), cryptograms and stem-associated microbial CH_4 oxidation (Feng et al., 2022; Jeffrey et al., 2021a; Jeffrey et al., 2021b; Machacova et al., 2021) and the net canopy exchange of CH_4 (Takahashi et al., 2021) should also be taken into account, in any mass balance and net ecosystem CH_4 flux estimates.

Currently, there is far less data available from the (sub)tropical ecosystems (hotspots for wetland CH_4 emissions), compared to lowland forests of higher latitudes. In the context of local and national greenhouse gas budgets, climate change mitigation and re-forestation efforts, constraining the role of tree stem CH_4 emissions from these important ecosystems requires considerable further research. Although recently identified as a knowledge and data gap that may potentially help explain the large uncertainties in the global CH_4 budget wetland term (Pachauri et al., 2014; Saunois et al., 2020), tree stem CH_4 emissions do not yet have a distinct emission category, nor are they used in bottom-up scaling and modelling efforts. As the drivers of tree stem CH_4 are highly dynamic and variable across ecosystem types and individual tree species, future modelling efforts will need to consider these complexities in any up-scaling approaches.

Acknowledgements: We thank Judith Rosentreter, Sebastian Euler, Bean Tait, Amy Jeffrey and Evan Jeffrey for fieldwork assistance, and Iain Alexander, Matt Veness, Ros Hagan and Peter Bligh-Jones for laboratory assistance. We acknowledge support and permission from

Tweed Shire Council and NSW NPWS. We also acknowledge and pay respects the Bundjalung people as the Traditional Custodians of the land on which this research occurred. This project was funded with support from the ARC (DP210100096, LP160100061), and The Hermon Slade Foundation. LJ's salary is funded by the ARC (DP210100096).

Data Availability Statement: The data used in this publication is freely available online via a Mendeley repository at https://data.mendeley.com/datasets/thdjfdmg8v/1

References

Aben, R. C. H., Barros, N., van Donk, E., Frenken, T., Hilt, S., Kazanjian, G., Lamers, L. P. M., Peeters, E., Roelofs, J. G. M., de Senerpont Domis, L. N., Stephan, S., Velthuis, M., Van de Waal, D. B., Wik, M., Thornton, B. F., Wilkinson, J., DelSontro, T., & Kosten, S. (2017). Cross continental increase in methane ebullition under climate change. *Nature Communication*, *8*(1), 1682. https://doi.org/10.1038/s41467-017-01535-y

Barba, J., Bradford, M. A., Brewer, P. E., Bruhn, D., Covey, K., van Haren, J., Megonigal, J. P., Mikkelsen, T. N., Pangala, S. R., & Pihlatie, M. (2019a). Methane emissions from tree stems: a new frontier in the global carbon cycle. *New Phytologist*, *222*(1), 18-28.

Barba, J., Poyatos, R., & Vargas, R. (2019b). Automated measurements of greenhouse gases fluxes from tree stems and soils: magnitudes, patterns and drivers. *Scientific Reports*, *9*(1), 4005. https://doi.org/10.1038/s41598-019-39663-8

Barbosa, P. M., Farjalla, V. F., Melack, J. M., Amaral, J. H. F., da Silva, J. S., & Forsberg, B. R. (2018). High rates of methane oxidation in an Amazon floodplain lake. *Biogeochemistry*, *137*(3), 351-365. https://doi.org/10.1007/s10533-018-0425-2

Bartlett, K. B., & Harriss, R. C. (1993). Review and assessment of methane emissions from wetlands. *Chemosphere*, *26*(1-4), 261-320.

Bureau of Meteorology - BOM (2023a). *Daily weather observations for Coolangatta.* http://www.bom.gov.au/climate/dwo/IDCJDW4036.latest.shtml (retrieved 6th April 2023).

Bureau of Meteorology – BOM (2023b). *ENSO Outlook.* http://www.bom.gov.au/climate/enso/outlook/ (retrieved 6th April 2023).

Boon, P. I., & Sorrell, B. K. (1995). Methane fluxes from an Australian floodplain wetland: the importance of emergent macrophytes. *Journal of the North American Benthological Society*, *14*(4), 582-598.

Borges, A. V., Darchambeau, F., Teodoru, C. R., Marwick, T. R., Tamooh, F., Geeraert, N., Omengo, F. O., Guérin, F., Lambert, T., & Morana, C. (2015). Globally significant greenhouse-gas emissions from African inland waters. *Nature Geoscience*, *8*(8), 637.

Brechet, L. M., Daniel, W., Stahl, C., Burban, B., Goret, J. Y., Salomón, R. L., & Janssens, I. A. (2021). Simultaneous tree stem and soil greenhouse gas (CO_2, CH_4, N_2O) flux

measurements: a novel design for continuous monitoring towards improving flux estimates and temporal resolution. *New Phytologist*, *230*(6), 2487-2500.

Bringel, F., & Couée, I. (2015). Pivotal roles of phyllosphere microorganisms at the interface between plant functioning and atmospheric trace gas dynamics [Review]. *Frontiers in microbiology*, *6*. https://doi.org/10.3389/fmicb.2015.00486

CABI, (2023). *Melaleuca quinquenervia (paperbark tree) data sheet.* https://www.cabi.org/isc/datasheet/34348 (retrieved 1st July 2023).

Carmichael, M. J., Bernhardt, E. S., Bräuer, S. L., & Smith, W. K. (2014). The role of vegetation in methane flux to the atmosphere: should vegetation be included as a distinct category in the global methane budget? *Biogeochemistry*, *119*(1-3), 1-24. https://doi.org/10.1007/s10533-014-9974-1

Carmichael, M. J., & Smith, W. K. (2016). Standing Dead Trees: a Conduit for the Atmospheric Flux of Greenhouse Gases from Wetlands? [journal article]. *Wetlands*, *36*(6), 1183-1188. https://doi.org/10.1007/s13157-016-0845-5

Center, T. D., Purcell, M. F., Pratt, P. D., Rayamajhi, M. B., Tipping, P. W., Wright, S. A., & Dray Jr, F. A. (2012). Biological control of Melaleuca quinquenervia: an Everglades invader. *BioControl*, *57*(2), 151-165.

Chanton, J. P., Martens, C. S., & Kelley, C. A. (1989). Gas transport from methane-saturated, tidal freshwater and wetland sediments. *Limnology and Oceanography*, *34*(5), 807-819.

Chiang, S.-H. T., & Wang, S.-c. (1984). The structure and formation of melaleuca bark. *Wood and Fiber Science*, 357-373.

Covey, K. R., & Megonigal, J. P. (2019). Methane production and emissions in trees and forests. *New Phytologist*, *222*(1), 35-51. https://doi.org/10.1111/nph.15624

Daniel, W., Stahl, C., Burban, B., Goret, J.-Y., Cazal, J., Richter, A., Janssens, I. A., & Bréchet, L. M. (2023). Tree stem and soil methane and nitrous oxide fluxes, but not carbon dioxide fluxes, switch sign along a topographic gradient in a tropical forest. *Plant and Soil*, 1-17.

DelSontro, T., Boutet, L., St-Pierre, A., del Giorgio, P. A., & Prairie, Y. T. (2016). Methane ebullition and diffusion from northern ponds and lakes regulated by the interaction between temperature and system productivity. *Limnology and Oceanography*, *61*(S1).

824 Feng, H., Guo, J., Ma, X., Han, M., Kneeshaw, D., Sun, H., Malghani, S., Chen, H., & Wang,
825 W. (2022). Methane emissions may be driven by hydrogenotrophic methanogens
826 inhabiting the stem tissues of poplar. *New Phytologist*, *233*(1), 182-193.
827 Flanagan, L. B., Nikkel, D. J., Scherloski, L. M., Tkach, R. E., Smits, K. M., Selinger, L. B.,
828 & Rood, S. B. (2021). Multiple processes contribute to methane emission in a riparian
829 cottonwood forest ecosystem. *New Phytologist*, *229*(4), 1970-1982.
830 Fuss, R. (2019). Gasfluxes: greenhouse gas flux calculation from chamber measurements. R
831 package version 0.4-3. In.
832 Gao, C.-H., Zhang, S., Ding, Q.-S., Wei, M.-Y., Li, H., Li, J., Wen, C., Gao, G.-F., Liu, Y., &
833 Zhou, J.-J. (2021). Source or sink? A study on the methane flux from mangroves
834 stems in Zhangjiang estuary, southeast coast of China. *Science of the Total*
835 *Environment*, *788*, 147782.
836 Gauci, V., Figueiredo, V., Gedney, N., Pangala, S. R., Stauffer, T., Weedon, G. P., & Enrich-
837 Prast, A. (2022). Non-flooded riparian Amazon trees are a regionally significant
838 methane source. *Philosophical Transactions of the Royal Society A*, *380*(2215),
839 20200446.
840 Gauci, V., Gowing, D. J., Hornibrook, E. R., Davis, J. M., & Dise, N. B. (2010). Woody stem
841 methane emission in mature wetland alder trees. *Atmospheric Environment*, *44*(17),
842 2157-2160.
843 Gorgolewski, A. S., Vantellingen, J., Caspersen, J. P., & Thomas, S. C. (2022). Overlooked
844 sources of methane emissions from trees: branches and wounds. *Canadian Journal of*
845 *Forest Research*, *52*(8), 1165-1175.
846 Iram, N., Maher, D. T., Lovelock, C. E., Baker, T., Cadier, C., & Adame, M. F. (2022).
847 Climate change mitigation and improvement of water quality from the restoration of a
848 subtropical coastal wetland. *Ecological Applications*, *32*(5), e2620.
849 Jeffrey, L. C., Maher, D. T., Chiri, E., Leung, P. M., Nauer, P. A., Arndt, S. K., Tait, D. R.,
850 Greening, C., & Johnston, S. G. (2021a). Bark-dwelling methanotrophic bacteria
851 decrease methane emissions from trees. *Nature Communications*, *12*(1), 2127.
852 https://doi.org/10.1038/s41467-021-22333-7
853 Jeffrey, L. C., Maher, D. T., Johnston, S. G., Kelaher, B. P., Steven, A., & Tait, D. R.
854 (2019a). Wetland methane emissions dominated by plant-mediated fluxes:
855 Contrasting emissions pathways and seasons within a shallow freshwater subtropical
856 wetland. *Limnology and Oceanography*. https://doi.org/10.1002/lno.11158

857 Jeffrey, L. C., Maher, D. T., Tait, D. R., Euler, S., & Johnston, S. G. (2020a). Tree stem
858 methane emissions from subtropical lowland forest (Melaleuca quinquenervia)
859 regulated by local and seasonal hydrology. *Biogeochemistry*, *151*(2), 273-290.
860 Jeffrey, L. C., Maher, D. T., Tait, D. R., & Johnston, S. G. (2020b). A Small Nimble In Situ
861 Fine-Scale Flux Method for Measuring Tree Stem Greenhouse Gas Emissions and
862 Processes (S.N.I.F.F). *Ecosystems*, *23*(8), 1676-1689. https://doi.org/10.1007/s10021-
863 020-00496-6
864 Jeffrey, L. C., Maher, D. T., Tait, D. R., Reading, M. J., Chiri, E., Greening, C., & Johnston,
865 S. G. (2021b). Isotopic evidence for axial tree stem methane oxidation within
866 subtropical lowland forests. *New Phytologist*, *230*(6), 2200-2212.
867 https://doi.org/https://doi.org/10.1111/nph.17343
868 Jeffrey, L. C., Reithmaier, G., Sippo, J. Z., Johnston, S. G., Tait, D. R., Harada, Y., & Maher,
869 D. T. (2019b). Are methane emissions from mangrove stems a cryptic carbon loss
870 pathway? Insights from a catastrophic forest mortality. *New Phytologist*, *224*(1), 146-
871 154. https://doi.org/https://doi.org/10.1111/nph.15995
872 Johnston, S. G., Slavich, P. G., & Hirst, P. (2003). Alteration of groundwater and sediment
873 geochemistry in a sulfidic backswamp due to Melaleuca quinquenervia encroachment.
874 *Soil Research*, *41*(7). https://doi.org/10.1071/sr03027
875 Kirschke, S., Bousquet, P., Ciais, P., Saunois, M., Canadell, J. G., Dlugokencky, E. J.,
876 Bergamaschi, P., Bergmann, D., Blake, D. R., Bruhwiler, L., Cameron-Smith, P.,
877 Castaldi, S., Chevallier, F., Feng, L., Fraser, A., Heimann, M., Hodson, E. L.,
878 Houweling, S., Josse, B., . . . Zeng, G. (2013). Three decades of global methane
879 sources and sinks. *Nature Geoscience*, *6*(10), 813-823.
880 https://doi.org/10.1038/ngeo1955
881 Lenhart, K., Bunge, M., Ratering, S., Neu, T. R., Schüttmann, I., Greule, M., Kammann, C.,
882 Schnell, S., Müller, C., Zorn, H., & Keppler, F. (2012). Evidence for methane
883 production by saprotrophic fungi [Article]. *Nature Communications*, *3*, 1046.
884 https://doi.org/10.1038/ncomms2049
885 Lovelock, C. E., Adame, M. F., Bradley, J., Dittmann, S., Hagger, V., Hickey, S. M., Hutley,
886 L. B., Jones, A., Kelleway, J. J., & Lavery, P. S. (2022). An Australian blue carbon
887 method to estimate climate change mitigation benefits of coastal wetland restoration.
888 *Restoration Ecology*, e13739.

Machacova, K., Back, J., Vanhatalo, A., Halmeenmaki, E., Kolari, P., Mammarella, I., Pumpanen, J., Acosta, M., Urban, O., & Pihlatie, M. (2016). Pinus sylvestris as a missing source of nitrous oxide and methane in boreal forest. *Scientific Reports*, *6*, 23410. https://doi.org/10.1038/srep23410

Machacova, K., Borak, L., Agyei, T., Schindler, T., Soosaar, K., Mander, Ü., & Ah-Peng, C. (2021). Trees as net sinks for methane (CH_4) and nitrous oxide (N_2O) in the lowland tropical rain forest on volcanic Réunion Island. *New Phytologist*, *229*(4), 1983-1994. https://doi.org/https://doi.org/10.1111/nph.17002

Machacova, K., Warlo, H., Svobodová, K., Agyei, T., Uchytilová, T., Horáček, P., & Lang, F. (2023). Methane emission from stems of European beech (Fagus sylvatica) offsets as much as half of methane oxidation in soil. *New Phytologist*.

Martinez, M., & Ardon, M. (2021). Drivers of greenhouse gas emissions from standing dead trees in ghost forests. *Biogeochemistry*, 1-18.

Masson-Delmotte, V., Zhai, P., Pirani, A., Connors, S. L., Péan, C., Berger, S., Caud, N., Chen, Y., Goldfarb, L., & Gomis, M. (2021). Climate change 2021: the physical science basis. *Contribution of working group I to the sixth assessment report of the intergovernmental panel on climate change*, *2*.

McJannet, D. (2008). Water table and transpiration dynamics in a seasonally inundated Melaleuca quinquenervia forest, north Queensland, Australia. *Hydrological Processes: An International Journal*, *22*(16), 3079-3090.

Megonigal, J. P., Brewer, P. E., & Knee, K. L. (2019). Radon as a natural tracer of gas transport through trees. *New phytologist*. *225*: 1470-1475. https://doi.org/10.1111/nph.16292

Moldaschl, E., Kitzler, B., Machacova, K., Schindler, T., & Schindlbacher, A. (2021). Stem CH_4 and N_2O fluxes of Fraxinus excelsior and Populus alba trees along a flooding gradient. *Plant and Soil*, *461*, 407-420.

Neubauer, S. C., & Megonigal, J. P. (2015). Moving beyond global warming potentials to quantify the climatic role of ecosystems. *Ecosystems*, *18*(6), 1000-1013.

Pachauri, R. K., Allen, M. R., Barros, V. R., Broome, J., Cramer, W., Christ, R., Church, J. A., Clarke, L., Dahe, Q., & Dasgupta, P. (2014). *Climate change 2014: synthesis report. Contribution of Working Groups I, II and III to the fifth assessment report of the Intergovernmental Panel on Climate Change*. Ipcc.

Pangala, S. R., Enrich-Prast, A., Basso, L. S., Peixoto, R. B., Bastviken, D., Hornibrook, E. R., Gatti, L. V., Marotta, H., Calazans, L. S. B., & Sakuragui, C. M. (2017). Large

emissions from floodplain trees close the Amazon methane budget. *Nature*, *552*(7684), 230.

Pangala, S. R., Gowing, D. J., Hornibrook, E. R., & Gauci, V. (2014). Controls on methane emissions from Alnus glutinosa saplings. *New Phytologist*, *201*(3), 887-896. https://doi.org/10.1111/nph.12561

Pangala, S. R., Moore, S., Hornibrook, E. R., & Gauci, V. (2013). Trees are major conduits for methane egress from tropical forested wetlands. *New Phytologist*, *197*(2), 524-531.

Peng, S., Lin, X., Thompson, R. L., Xi, Y., Liu, G., Hauglustaine, D., Lan, X., Poulter, B., Ramonet, M., & Saunois, M. (2022). Wetland emission and atmospheric sink changes explain methane growth in 2020. *Nature*, *612*(7940), 477-482.

Pitz, S., & Megonigal, J. P. (2017). Temperate forest methane sink diminished by tree emissions. *New Phytologist*, *214*(4), 1432-1439.

Pitz, S. L., Megonigal, J. P., Chang, C.-H., & Szlavecz, K. (2018). Methane fluxes from tree stems and soils along a habitat gradient. *Biogeochemistry*, *137*(3), 307-320.

Plain, C., & Epron, D. (2021). Pulse labelling of deep soil layers in forest with 13 CH 4: testing a new method for tracing methane in the upper horizons, understorey vegetation and tree stems using laser-based spectrometry. *Biogeochemistry*, *153*(2), 215-222.

Putkinen, A., Siljanen, H. M., Laihonen, A., Paasisalo, I., Porkka, K., Tiirola, M., Haikarainen, I., Tenhovirta, S., & Pihlatie, M. (2021). New insight to the role of microbes in the methane exchange in trees: evidence from metagenomic sequencing. *New Phytologist*.

Roberts, H. M., & Shiller, A. M. (2015). Determination of dissolved methane in natural waters using headspace analysis with cavity ring-down spectroscopy. *Analytica chimica acta*, *856*, 68-73.

Sakabe, A., Takahashi, K., Azuma, W., Itoh, M., Tateishi, M., & Kosugi, Y. (2021). Controlling factors of seasonal variation of stem methane emissions from Alnus japonica in a riparian wetland of a temperate forest. *Journal of Geophysical Research: Biogeosciences*, *126*(10), e2021JG006326.

Saunois, M., Jackson, R. B., Bousquet, P., Poulter, B., & Canadell, J. G. (2016). The growing role of methane in anthropogenic climate change. *Environmental Research Letters*, *11*(12), 120207. https://doi.org/10.1088/1748-9326/11/12/120207

Saunois, M., Stavert, A. R., Poulter, B., Bousquet, P., Canadell, J. G., Jackson, R. B., Raymond, P. A., Dlugokencky, E. J., Houweling, S., & Patra, P. K. (2020). The global methane budget 2000–2017. *Earth System Science Data*, *12*(3), 1561-1623.

Siegenthaler, A., Welch, B., Pangala, S. R., Peacock, M., & Gauci, V. (2016). Technical Note: Semi-rigid chambers for methane gas flux measurements on tree stems. *Biogeosciences*, *13*(4), 1197-1207. https://doi.org/10.5194/bg-13-1197-2016

Sjögersten, S., Siegenthaler, A., Lopez, O. R., Aplin, P., Turner, B., & Gauci, V. (2020). Methane emissions from tree stems in neotropical peatlands. *New Phytologist*, *225*(2), 769-781. https://doi.org/https://doi.org/10.1111/nph.16178

Smits, K. M., Grant, D. S., Johnston, S. E., Bogard, M. J., Rood, S. B., Selinger, L. B., & Flanagan, L. B. (2021). Riparian cottonwood trees and adjacent river sediments have different microbial communities and produce methane with contrasting carbon isotope compositions. *Journal of Geophysical Research: Biogeosciences*, e2021JG006699.

Takahashi, K., Sakabe, A., Kanazawa, A., & Kosugi, Y. (2021). Vertical profiles of methane concentration above and within the canopy of a temperate Japanese cypress forest. *Atmospheric Environment: X*, *12*, 100143.

Terazawa, K., Ishizuka, S., Sakata, T., Yamada, K., & Takahashi, M. (2007). Methane emissions from stems of Fraxinus mandshurica var. japonica trees in a floodplain forest. *Soil Biology and Biochemistry*, *39*(10), 2689-2692.

Terazawa, K., Tokida, T., Sakata, T., Yamada, K., & Ishizuka, S. (2021). Seasonal and weather-related controls on methane emissions from the stems of mature trees in a cool-temperate forested wetland. *Biogeochemistry*, *156*(2), 211-230.

Van Stan, J. T., Dymond, S. F., & Klamerus-Iwan, A. (2021). Bark-Water Interactions Across Ecosystem States and Fluxes [Perspective]. *Frontiers in Forests and Global Change*, *4*. https://doi.org/10.3389/ffgc.2021.660662

Wang, Z.-P., Li, H.-L., Wu, H.-H., Han, S.-J., Huang, J.-H., Zhang, X.-M., & Han, X.-G. (2021). Methane concentration in the heartwood of living trees and estimated methane emission on stems in upland forests. *Ecosystems*, 1-15.

Wang, Z. P., Gu, Q., Deng, F. D., Huang, J. H., Megonigal, J. P., Yu, Q., Lu, X. T., Li, L. H., Chang, S., Zhang, Y. H., Feng, J. C., & Han, X. G. (2016). Methane emissions from the trunks of living trees on upland soils. *New Phytologist*, *211*(2), 429-439. https://doi.org/10.1111/nph.13909

Warner, D. L., Villarreal, S., McWilliams, K., Inamdar, S., & Vargas, R. (2017). Carbon dioxide and methane fluxes from tree stems, coarse woody debris, and soils in an upland temperate forest. *Ecosystems*, *20*(6), 1205-1216.

Wiesenburg, D. A., & Guinasso Jr, N. L. (1979). Equilibrium solubilities of methane, carbon monoxide, and hydrogen in water and sea water. *Journal of Chemical and Engineering Data*, *24*(4), 356-360.

Yip, D. Z., Veach, A. M., Yang, Z. K., Cregger, M. A., & Schadt, C. W. (2019). Methanogenic Archaea dominate mature heartwood habitats of Eastern Cottonwood (Populus deltoides). *New Phytologist*, *222*(1), 115-121.

Zeikus, J., & Ward, J. (1974). Methane formation in living trees: a microbial origin. *Science*, *184*(4142), 1181-1183.

Zhang, C., Zhang, Y., Luo, M., Tan, J., Chen, X., Tan, F., & Huang, J. (2022). Massive methane emission from tree stems and pneumatophores in a subtropical mangrove wetland. *Plant and Soil*, *473*(1-2), 489-505.

List of Figures

Figure 1. Map of study site in the upper panel showing locations of sampled *Melaleuca* trees (red, yellow and green dots), the location of water level loggers (white dots). The lower panel shows hydro-topological zones and tree base elevational differences relative to the lowest location in the wetland forest (black squares).

Figure 2. Summary of environmental conditions during the eight study campaigns showing seasonal changes in the Lower zone wetland water table (cm), daily rainfall totals (mm), maximum and minimum air temperature (°C) and photosynthetically available radiation (PAR in lum m^{-2}). Note: Dry campaigns are highlighted in grey.

Figure 3. Depth profiles for porewater and surface water CH_4 concentrations (μM) during campaigns 4-7 for each wetland zone. Note: Different x-axis scales used. The brown shaded area represents the soil and blue area is surface water and dashed line is the top of water table. Error bars are SE.

Figure 4. Stacked plots indicating the changing water table within each zone, average CH_4 flux per tree (mmol $tree^{-1}$ d^{-1}) and average CH_4 flux from water or soil (mmol m^{-2} d^{-1}). Note: Different y-axis scales, shaded campaigns are where surface water was present, the horizontal dashed line is soil surface, the horizontal solid line separates CH_4 sink and source in Upper zone. Error bars are SE.

Figure 5. Contour plots showing average tree stem CH_4 flux rates (mmol m^{-2} d^{-1}) at each stem height, from each campaign and within each hydro-topographic zone. Note: log scale of CH_4 flux rates (mmol m^{-2} d^{-1}) and water table is from the Lower zone and the dashed line is the soil surface.

Figure 6. Positive significant correlations between soil WVC% and lower (10-40 cm) tree stem CH_4 fluxes during the three Dry campaigns. Note: log scale y-axis, Spearman's Rho (r_s), grey areas show 99 % confidence interval and 50% VWC is the upper volumetric water content range of the probe.

Figure 7. Correlations between lower (10-40 cm) tree stem CH_4 fluxes and a) soil CH_4 fluxes (Dry campaigns) and b) aquatic CH_4 fluxes (Wet campaigns) within the Lower and Transitional hydro-topological zones. Note: Spearman's Rho (r_s) and grey areas show 99 % confidence interval.

Figure 8. Correlations for all positive tree stem CH_4 flux data vs **(a)** chamber height distance from water table during Dry campaigns, and **(b)** chamber heights above soil surface during Wet campaigns. Note: Log transformed data on y-axis. Yellow lines are 95 % confidence intervals and dashed lines are 95 % prediction intervals.

Figure 9. Upscaled wetland CH_4 NEF differentiating the CH_4 flux from tree stems, water and soils from each hydro-topological zone and campaign (mol ha^{-1} d^{-1}). The values above bar plots indicate the tree CH_4 contribution to: (1) the NEF % (black text); (2) offsetting soil CH_4 uptake (blue text), and (3) enhancing soil uptake (red text). Note: different y-axis scales.

Figure 10. Regression of lower stem tree stem fluxes (10 and 40 cm) vs water table height below the soil surface (Dry campaigns) and above the soil surface (Wet campaigns). Note: Log scale and data for Lower and Transitional zones only. The grey shaded area is the 99 % confidence interval.

Figure 11. Conceptual summary diagram of the net ecosystem CH_4 flux from trees (NEF, %) during Wet campaigns (n=5), Dry campaigns (n=3) and annual emissions (n=8). The average CH_4 flux rates for each pathway (mmol m^{-2} d^{-1}) are shown with arrow size depicting the scale of emissions.

Figure 12. Comparison of previously reported tree stem ecosystem CH_4 flux rates spanning various forest types (Covey & Megonigal, 2019; Jeffrey et al., 2020a; Jeffrey et al., 2019b; Sjögersten et al., 2020) compared to the average, Wet and Dry tree CH_4 emissions of our study. Note: The log scale on the y-axis.

Figure 1.

153.570898°E

153.572868°E

28.349502°S

28.351530°S

Bogangar

Tweed Coast Rd

Pacific Ocean

N

100 m

Water level loggers
Upper zone
Transitional zone
Lower zone
Max. flood areal extent

Lower zone

Transitional zone

Upper zone

Elevation relative to lowest tree base (cm)

280

210

140

70

0

Max water height

Min water height

L30 L29 L28 L27 L26 L25 L24 L23 L22 L21 T20 T19 T18 T17 T16 T15 T14 T13 T12 T11 U10 U9 U8 U7 U6 U5 U4 U3 U2 U1

Melaleuca tree ID

Figure 2.

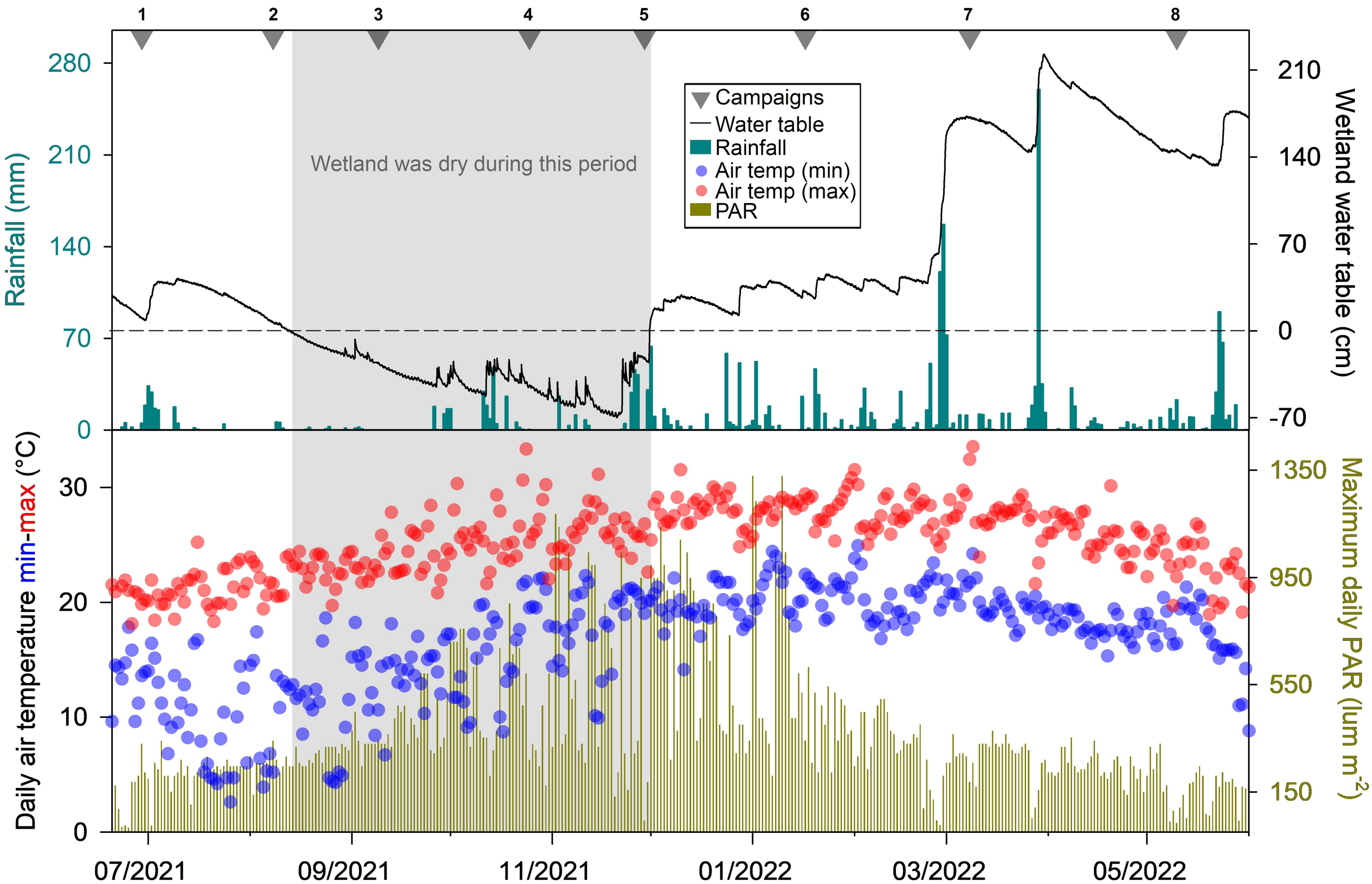
1
2
3
4
5
6
7
8
Wetland was dry during this period
Campaigns
Water table
Rainfall
Air temp (min)
Air temp (max)
PAR
Rainfall (mm)
280
210
140
70
0
Wetland water table (cm)
210
140
70
0
-70
Daily air temperature min-max (°C)
30
20
10
0
Maximum daily PAR (lum m-2)
1350
950
550
150
07/2021
09/2021
11/2021
01/2022
03/2022
05/2022

Figure 3.

Lower zone

Transitional zone

Upper zone

Campaign 4

Campaign 5

Campaign 6

Campaign 7

Wetland depth above and below soil (cm)

Aquatic CH_4 (μM)

Figure 4.

Lower zone

Transitional zone

Upper zone

Water table (cm)

200
100
0
-100
-200

Jul Sep Nov Jan Mar May

Tree stem CH_4 flux (mmol tree^{-1} d^{-1})

100
10
1
0.1

4
3
2
1
0

Water and soil CH_4 flux (mmol m^{-2} d^{-1})

100
0
1
0.1
10

-0.02

1.5
1.2
0.9
0.1
0.0
-0.1

Figure 5.

Field campaigns

1 2 3 4 5 6 7 8

Tree stem measurement height (cm)

Upper

Transitional

Lower

CH_4 flux
0.01
0.1
1
10
100

Average water table (cm)

Water level

Soil surface

07/2021 09/2021 11/2021 01/2022 03/2022 05/2022

Figure 6.

Campaign 3
r_s=0.742
p<0.001
n=30

Campaign 4
r_s=0.882
p<0.001
n=30

Campaign 5
r_s=0.835
p<0.001
n=26

Combined data
r_s=0.838
p<0.001
n=86

Lower stem CH_4 flux (mmol m^{-2} d^{-1})

Soil moisture (VWC %)

Figure 7.

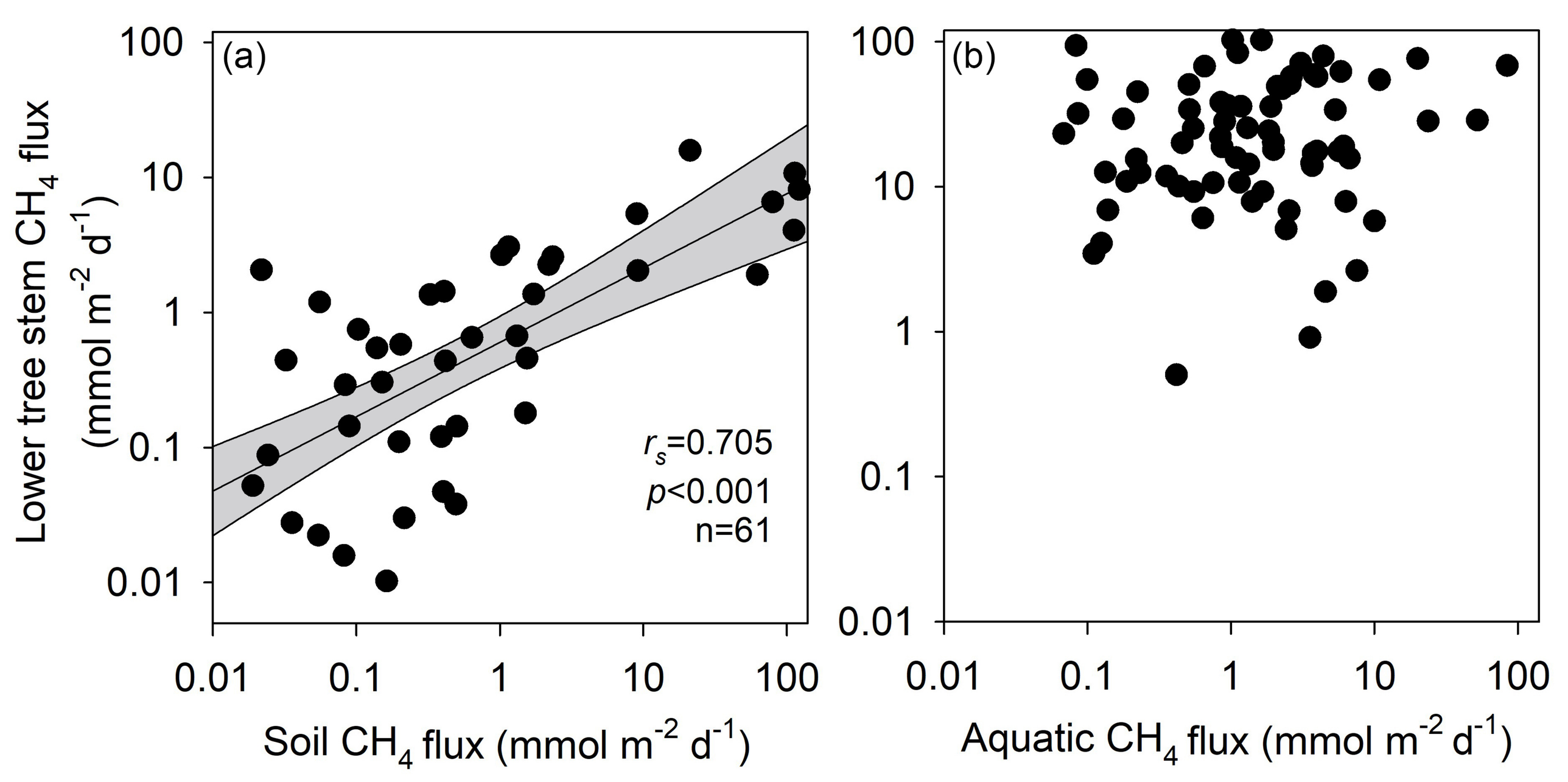
(a)
(b)
Lower tree stem CH_4 flux (mmol m^{-2} d^{-1})
Soil CH_4 flux (mmol m^{-2} d^{-1})
Aquatic CH_4 flux (mmol m^{-2} d^{-1})
r_s=0.705
p<0.001
n=61
100
10
1
0.1
0.01

Figure 8.

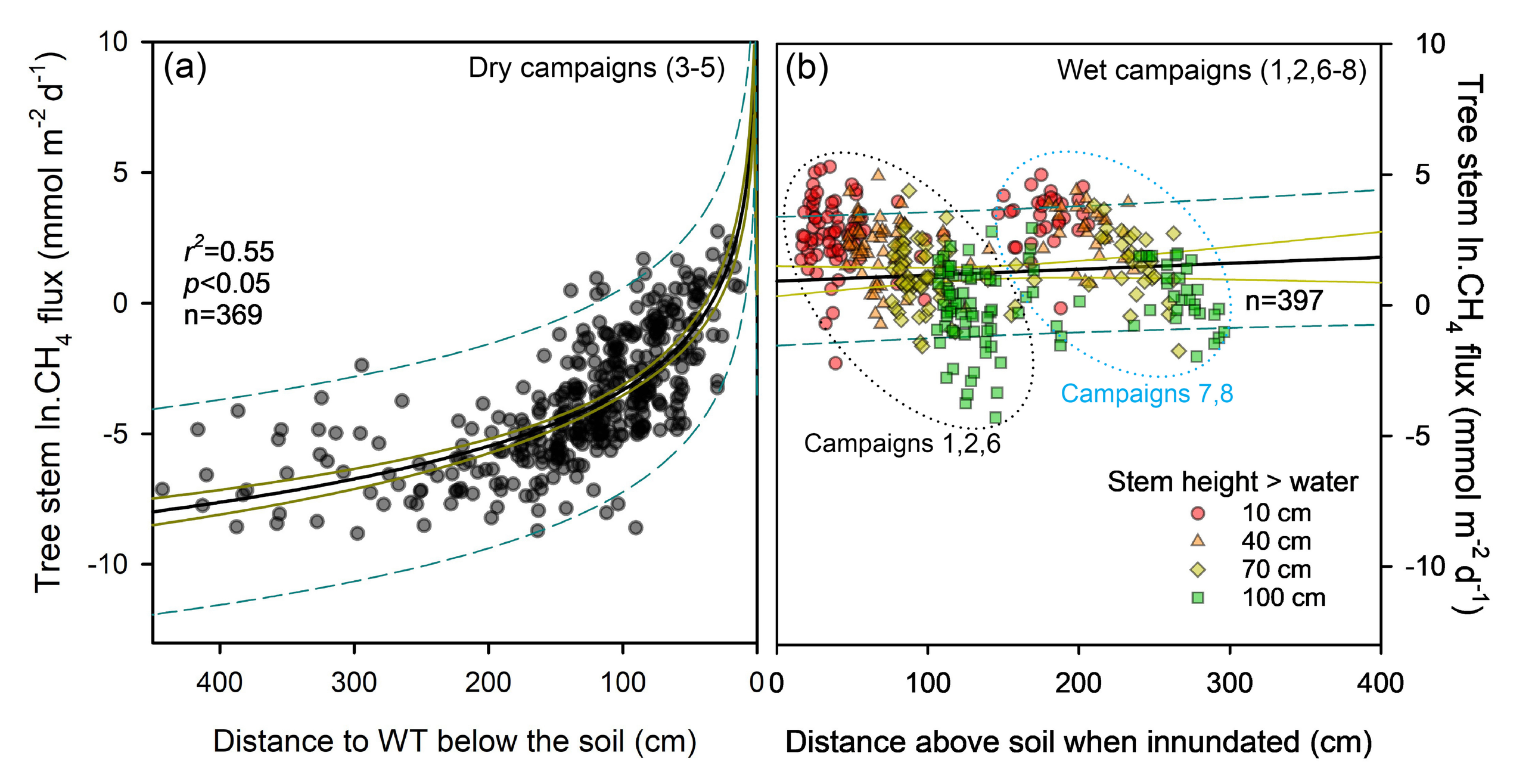
(a)
Dry campaigns (3-5)
r^2=0.55
p<0.05
n=369
(b)
Wet campaigns (1,2,6-8)
n=397
Campaigns 7,8
Campaigns 1,2,6
Stem height > water
10 cm
40 cm
70 cm
100 cm
Tree stem ln.CH4 flux (mmol m-2 d-1)
Tree stem ln.CH4 flux (mmol m-2 d-1)
Distance to WT below the soil (cm)
Distance above soil when innundated (cm)
10
5
0
-5
-10
400
300
200
100
0
0
100
200
300
400

Figure 9.

Upper zone

Transitional zone

Lower zone

Soil

Water

Trees

Wetland CH_4 flux (mol ha^{-1} d^{-1})

18

12

6

0

90

60

30

255

50

30

10

52%

(5%)

(31%)

1.9 x soil uptake

= soil uptake

2.1 x soil uptake

96%

52%

86%

62%

15%

35%

6.5 x soil uptake

47%

93%

85%

25%

49%

2%

51%

28%

63%

78%

46%

1 2 3 4 5 6 7 8

Campaigns

Figure 10.

Dry campaigns

Wet campaigns

r^2=0.41
p<0.001
n=247

r^2=0.01

Lower tree stem CH_4 flux (mmol m^{-2} d^{-1})

10^2
10^1
10^0
10^{-1}
10^{-2}
10^{-3}
10^{-4}

-120
-60
0
60
120
180

Water table (cm)

Campaigns
1
2
3
4
5
6
7
8

Figure 11.

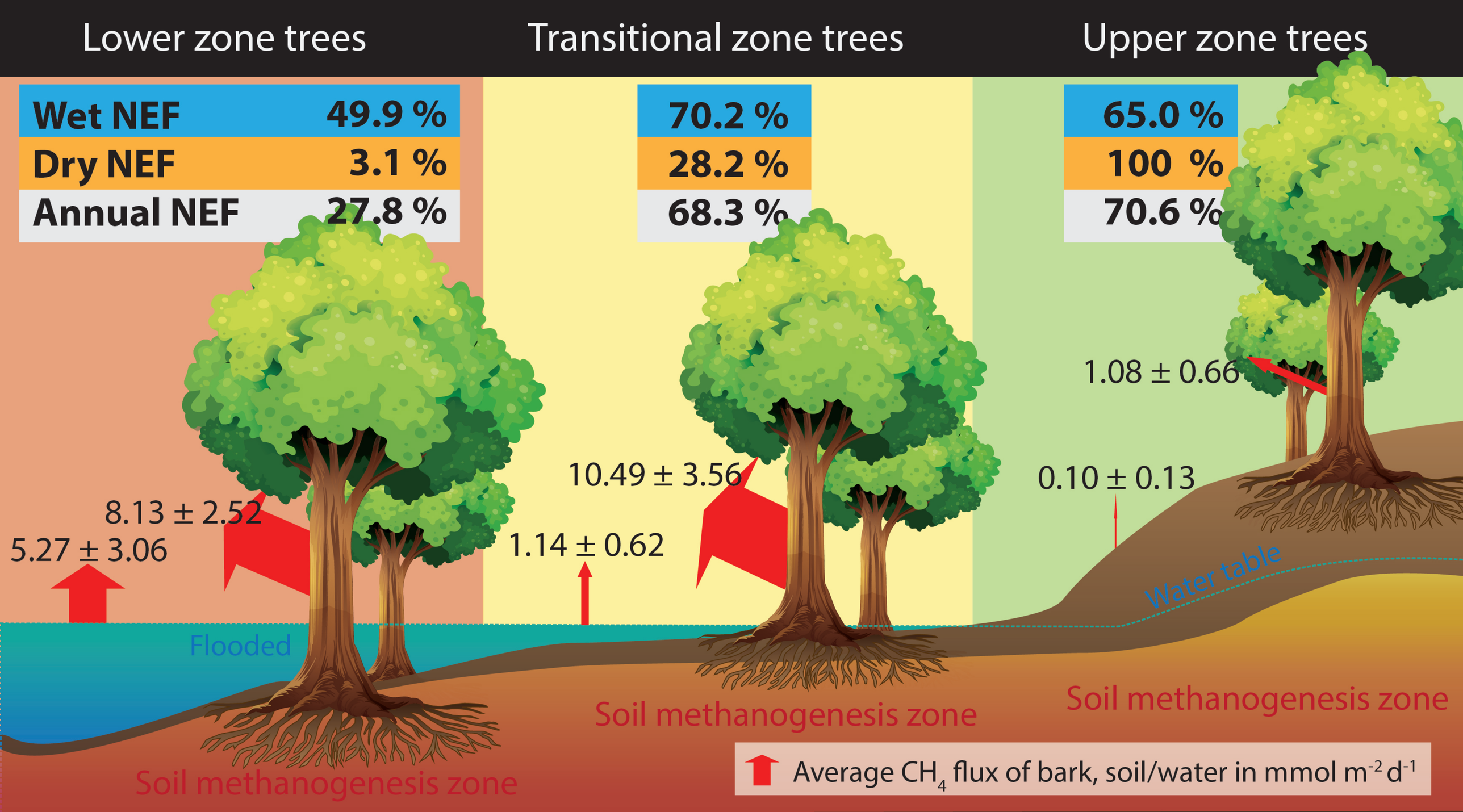
Lower zone trees
Transitional zone trees
Upper zone trees
Wet NEF 49.9 %
Dry NEF 3.1 %
Annual NEF 27.8 %
70.2 %
28.2 %
68.3 %
65.0 %
100 %
70.6 %
1.08 ± 0.66
0.10 ± 0.13
10.49 ± 3.56
8.13 ± 2.52
5.27 ± 3.06
1.14 ± 0.62
Water table
Flooded
Soil methanogenesis zone
Soil methanogenesis zone
Soil methanogenesis zone
Average CH_4 flux of bark, soil/water in mmol m^{-2} d^{-1}

Figure 12.

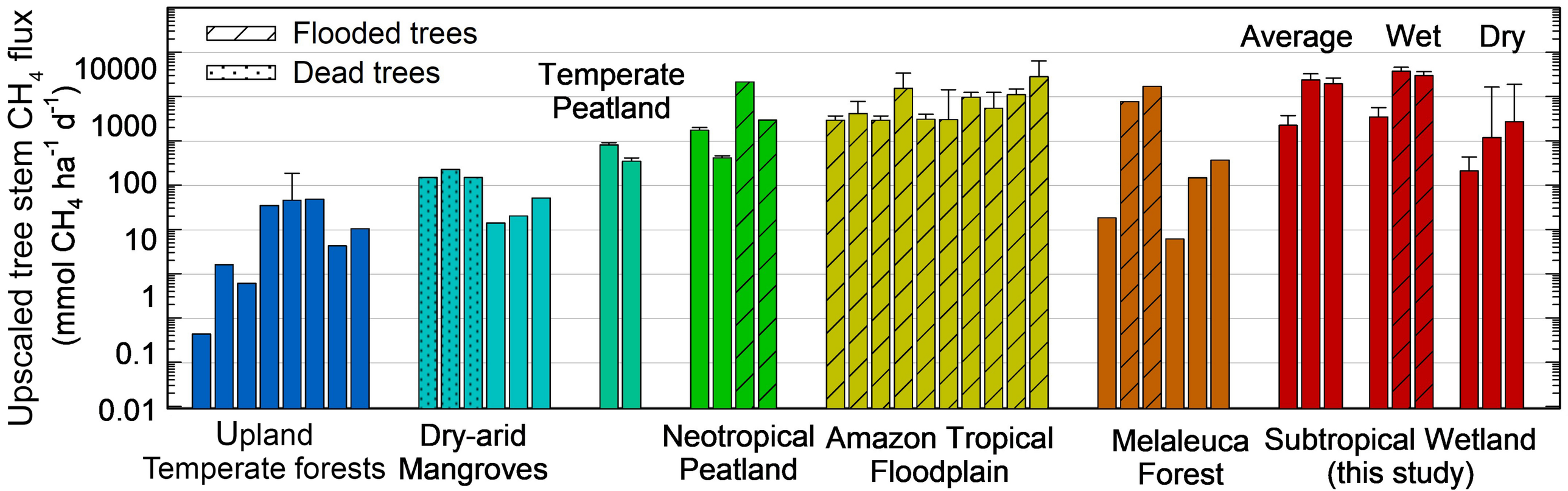
Upscaled tree stem CH_4 flux
(mmol CH_4 ha^{-1} d^{-1})
10000
1000
100
10
1
0.1
0.01
Flooded trees
Dead trees
Average
Wet
Dry
Temperate Peatland
Upland Temperate forests
Dry-arid Mangroves
Neotropical Peatland
Amazon Tropical Floodplain
Melaleuca Forest
Subtropical Wetland (this study)